Proteomic characterization of extracellular vesicles from 12 commensal bacterial species

Roselydiah Nasipwondi Makunja[1], Arina Maltseva[1], Tiina Pessa-Morikawa[1], Masuma Khatun[2], Johanna Muurinen[1], Maria[3], Mari Heinonen[4], Anna Kaisanlahti[5], Subhashini Muhandiram[6], Justus Reunanen[7], Terhi Ruuska-Loewald[5], Tuula Anneli Nyman[3], Mikael Niku[1*]*

1: Veterinary Biosciences, Faculty of Veterinary Medicine, University of Helsinki, Helsinki, Finland
2: Department of Obstetrics and Gynecology, University of Helsinki and Helsinki University Hospital, Helsinki, Finland
3: Department of Immunology and transfusion medicine, University of Oslo and University Hospital, Oslo, Norway.
4: Department of Production Animal Medicine, Faculty of Veterinary Medicine, University of Helsinki, Helsinki, Finland
5: Research Unit of Clinical Medicine and Biocenter Oulu, University of Oulu, and Department of Pediatrics and Adolescent Medicine, Oulu University Hospital, Oulu, Finland
6: Institute of Veterinary Medicine and Animal Sciences, Estonian University of Life Sciences, Tartu, Estonia
7: Research Unit of Translational Medicine and Biocenter Oulu, University of Oulu, Oulu, Finland

*Corresponding author

Funding: *This work was supported by the Research Council of Finland (grant number 347925), the European Union through HORIZON Coordination and Support Actions under grant agreement No 101079349 "OH-Boost", and the Finnish Foundation of Veterinary Research.*

Abstract

Bacterial extracellular vesicles (bEVs) produced by intestinal commensal bacteria mediate host-microbe interactions, but their proteomes have been explored in only a small number of species. We characterized bEVs from *in vitro* cultures of 12 species of Actinomycetota, Bacillota (Firmicutes), Bacteroidota, Fusobacteria, Pseudomonadota, and Verrucomicrobia. This is the first report of bEVs from *Veillonella magna*, an exceptional gram-negative Bacillota, and the gram-positives *Peptostreptococcus russellii* and *Turicibacter sanguinis*. The morphology and protein subcellular localization patterns of bEVs reflected the envelope structures of their parent bacteria. Notably, *V. magna* may be able to produce both outer membrane and cytoplasmic membrane vesicles. The proteome compositions were dictated by phylogeny, suggesting largely non-selective packaging of proteins. Annotation of protein functions indicated roles in nutrient

metabolism and transport, and in host immune system modulation. Peptidoglycan modifying enzymes and the abundant bacteriophage proteins in *Enterobacter cloacae* and *Limosilactobacillus reuteri* bEVs may be involved in vesicle biogenesis. The functions of many abundant bEV proteins are unknown. The most abundant bEV proteins were largely species-specific, but we identified several conserved proteins that may be used as markers to distinguish commensal bEVs from host EVs. Comparison to previous *in vitro* and fecal metaproteomics data indicates that bEV proteome compositions are reproducible.

Keywords

Bacterial extracellular vesicles, outer-membrane vesicles, gram-positive, gram-negative, proteome, intestinal commensal bacteria

Introduction

Bacterial extracellular vesicles (bEVs) are membrane-derived lipid bilayer nanoparticles, secreted by both gram-negative and gram-positive bacteria, ranging in size from 40 to 400 nm (1). Their biogenesis is influenced by the structure of the cell envelope, which differs between gram-negative and gram-positive bacteria (2, 3). In gram-negative bacteria, bEVs are secreted by outer membrane blebbing or phage-mediated explosive cell lysis, while in gram-positive bacteria, they are produced through budding or blebbing of the cytoplasmic membrane or phage-mediated bubbling cell death (1). The bEV cargo consists of proteins, nucleic acids, lipids, and small-molecular metabolites, which may be delivered to other microbial or host cells (4, 5). Compared to simple diffusion, bEVs can deliver highly concentrated signals over extended distances, referred to as quantal secretion (1). During transit, the cargo is protected from environmental inactivators and degrading enzymes (6).

In the intestine, commensal bEVs play diverse roles in bacteria-bacteria and bacteria-host interactions (7-9). They aid bacteria in nutrient acquisition, niche competition, and adaptation to environmental stress (10). bEVs carry enzymes that degrade complex carbohydrates, supporting the growth and survival of both the producer and other members of the microbial community (11). bEVs prime the host immune system against viral (12) and bacterial infections (13); they may have anti-inflammatory properties (14-16) and improve epithelial barrier integrity (14, 17). The immunomodulatory effects of bEVs may be even more potent than those of the producing bacteria since they can be internalized by host cells, thereby activating intracellular immune receptors (12, 18). Thus, bEVs hold promise for therapeutic applications, including immunotherapy, management of inflammatory bowel disease (IBD), cancer treatment, and drug delivery (4, 19, 20).

Commensal bEVs and especially their proteomes have only been characterized from a small part of the intestinal microbiota, with most studies focusing on a few bacterial species such as *Akkermansia muciniphila* (21-26), *Bacteroides fragilis* (18, 27-29), and *Bifidobacterium longum* (30, 31). They are usually studied *in vitro*, as *in vivo* research is complicated by a lack of markers for distinguishing bacterial from host extracellular vesicles (EVs) (4, 32). The growth conditions, bacterial strains, and bEV processing workflows may significantly influence the observed bEV composition (4, 19, 32, 33).

31 In the current study, we assessed the structures and proteomes of bEVs derived from gram-
32 negative and gram-positive commensal bacteria, representing all major phyla and orders of the
33 mammalian intestinal microbiota. We searched for conserved proteins that could serve as
34 markers for bEVs in animal samples. To assess the effects of bEV processing workflows and
35 experimental methods on the observed bEV characteristics, we compared our data to previous
36 bEV studies from the same bacterial species.

37

38 ## Materials and methods

39 The experimental protocol has been submitted to the EV-TRACK knowledgebase (EV-TRACK
40 ID: EV250029) (34).

41 ### Bacterial culture

42 The bacterial strains (Table 1) were obtained from culture collections, except for *Lactobacillus*
43 *amylovorus* and *Limosilactobacillus reuteri*, which were in-house isolates from sow feces
44 collected from Finnish pig farms (35). The cultured strains were verified by MALDI-TOF and/or
45 Sanger sequencing of the 16S rRNA genes.

46 The bacteria were cultured anaerobically at +37 °C, without shaking (Table 1). Most of the
47 bacteria were cultured in the Brain Heart Infusion broth (BHI; Merck Millipore #53286). For
48 some species indicated in the BHI medium was supplemented with yeast extract (5 g/l), hemin (5
49 mg/l), vitamin K (1 mg/l), cellobiose (1 g/l), maltose (1 g/l), and cysteine (1 g/l). *L. reuteri* and
50 *L. amylovorus* were cultured in deMan, Rogosa and Sharpe broth (MRS; Oxoid / Thermo Fisher
51 Scientific #CM0359). We also tested Gifu Anaerobic Medium (GAM; Nissui Pharmaceutical
52 #05433), but it contained high concentrations of EV-like particles and filtration resulted in poor
53 bacterial growth.

54 For the final 30 ml cultures (each species with three replicates) used for EV isolation, the culture
55 media were pre-filtered using 0.45 µm and 0.1 µm sterilization filters (Acrodisk Supor, Pall
56 Lab/Cytiva) to deplete EV-like particles. The EVs were collected when the cultures were clearly
57 cloudy (depending on bacterial strain, 1–4 days).

58 The following strains did not grow in our experimental conditions: *Alistipes senegalensis* (DSM
59 25460*)*, *Anaerostipes hadrus* (DSM 3319), *Eubacterium biforme* (DSM 3989), and *Prevotella*
60 *histicola* (DSM 26979).

61

62

63 **Table 1. Bacterial strains and culture media.** BHI: Brain Heart Infusion broth (BHI). BHI+:
64 BHI with supplements. MRS: deMan, Rogosa and Sharpe broth. The Bacillota phylum was
65 previously Firmicutes.

Phylum	Order	*Species*	Strain	Medium
Actinomycetota	Bifidobacteriales	*Bifidobacterium longum sp. suis*	DSM 20211	BHI
Actinomycetota	Coriobacteriia	*Collinsella aerofaciens*	DSM 3979	BHI+
Bacillota	Lactobacillales	*Enterococcus faecalis*	ATCC 29212	BHI
Bacillota	Lactobacillales	*Lactobacillus amylovorus*	in-house (35)	MRS
Bacillota	Lactobacillales	*Limosilactobacillus reuteri*	in-house (35)	MRS
Bacillota	Lactobacillales	*Streptococcus salivarius*	DSM 20067	BHI
Bacillota	Clostridiales	*Clostridium leptum*	DSM 753	BHI
Bacillota	Clostridiales	*Flavonifractor plautii*	DSM 4000	BHI
Bacillota	Eubacteriales	*Faecalibacterium prausnitzii*	DSM 107838	BHI+
Bacillota	Eubacteriales	*Peptostreptococcus russellii*	DSM 23041	BHI
Bacillota	Erysipelotrichales	*Turicibacter sanguinis*	DSM 14220	BHI
Bacillota	Erysipelotrichales	*Floccifex porci*	DSM 104670	BHI+
Bacillota	Erysipelotrichales	*Holdemanella biformis*	DSM 3989	BHI+
Bacillota	Veillonellales	*Veillonella magna*	DSM 19857	BHI
Bacteroidota	Bacteroidales	*Bacteroides fragilis*	DSM 2151	BHI
Pseudomonadota	Burkholderiales	*Escherichia coli*	ATCC 35328	BHI
Pseudomonadota	Burkholderiales	*Sutterella parvirubra*	DSM 19354	BHI+
Pseudomonadota	Enterobacteriales	*Enterobacter cloacae*	ATCC 13047	BHI
Verrucomicrobia	Verrucomicrobiales	*Akkermansia muciniphila*	DSM 22959	BHI
Fusobacteria	Fusobacteriales	*Fusobacterium nucleatum sp. animalis*	DSM 19679	BHI

66

67 Isolation of bacterial extracellular vesicles

68 Bacterial cells were removed by centrifugation for 10 min at 3100 × *g* (4000 rpm) using an
69 Eppendorf 5810 R Centrifuge, with swing-bucket rotor A-4-81. The supernatants were filtered
70 through a 0.22 µm sterilization filter (Millex-GP, Merck Millipore) using a peristaltic pump and
71 stored overnight at +4 °C. EVs were collected by ultracentrifugation of 3 × 22 ml culture
72 supernatant per species at 110000 × *g* for 2 hours at +4 °C, using Optima LE-80K ultracentrifuge
73 with a Ti 50.2 rotor, k-factor 143.3 (Beckman Coulter), and resuspended in 500 µl phosphate-
74 buffered saline (PBS, 0.22 µm pre-filtered). Size exclusion chromatography was performed
75 using 70 nm qEV Original columns (Izon Science). 500 µl per sample was loaded, and 3 × 0.5
76 ml fractions were collected by washing with PBS. Finally, samples were concentrated by
77 ultrafiltration at 3200 × *g* using 10 kDa MWCO 4 ml Amicon Ultra tubes (Merck), loading 1.5
78 ml per sample and collecting 100 µl.

79 ## Characterization of bacterial extracellular vesicles by NTA and electron microscopy

80 Particle concentration and size were measured with the ZetaView PMX-120 nanoparticle
81 tracking analysis (NTA) instrument (Particle Metrix GmbH, Ammersee, Germany) equipped
82 with a Z NTA cell assembly, a blue (488 nm, 40 mW) laser, and a CMOS camera with 640 x
83 480-pixel resolution. Samples were diluted in a total volume of 1 ml of particle-free ultra-pure
84 milli-Q water to obtain 50–200 particles per frame. Videos in NTA mode were recorded at 11
85 positions across the measurement chamber in two-second increments at 30 FPS framerate with
86 camera shutter speed at 100 s^{-1} and sensitivity at 85. The temperature was controlled at 22°C for
87 NTA. Videos were processed, and outliers (>10% CV) were removed using the Grubbs method
88 with the built-in ZetaView software (version 8.05.12 SP2). Particles between 10-1000 nm in
89 diameter with a minimum trace length of 15 frames and a minimum brightness of 20 were
90 included in the analysis. Culture media without bacteria were used as negative controls (nine
91 replicates of BHI medium, out of which one replicate was removed as an outlier due to much
92 higher particle concentration and different size range; and three replicates of MRS medium).

93 EVs were prepared for electron microscopy (EM) as in Puhka *et al*. (36) by loading to carbon-
94 coated and glow-discharged 200 mesh copper grids with a pioloform support membrane. EVs
95 were fixed with 2% paraformaldehyde in NaPO4 buffer, stained with 2% neutral uranyl acetate,
96 and further stained and embedded in uranyl acetate and methyl cellulose mixture (1.8/0.4 %).
97 EVs were viewed with transmission EM (TEM) using Jeol JEM-1400 (Jeol Ltd., Tokyo, Japan)
98 operating at 80 kV. Images were taken with Gatan Orius SC 1000B CCD-camera (Gatan Inc.,
99 USA) with 4008 × 2672 px image size and no binning.

100 ## LC-MS/MS analysis of bacterial extracellular vesicle proteomes

101 For the isolation and preparation of bEV proteins, a magnetic bead-based method was used for
102 most species. Here, the EV proteins were precipitated with 70% acetonitrile onto magnetic beads
103 (MagReSynAmine, Resyn Biosciences), and then washed on the beads with 100% acetonitrile,
104 70% ethanol, and then resuspended in 100 µl of 50 mM ammoniumbicarbonate. The proteins
105 were reduced by the addition of 0.5M DTT to a final concentration of 10 mM and incubation at
106 56°C for 30 min. To alkylate proteins, 2.7µl of 550 mM iodoacetamide (IAA) was added to a
107 final concentration of 15 mM, and samples were incubated at room temperature in the dark for
108 30 min. 0.5 µg trypsin was added to each sample for overnight on-beads protein digestion at
109 37°C. The resulting peptides were concentrated using the STAGE-TIP method with a C18 resin
110 disk (Affinisep).

111 An earlier non-bead-based protocol was used for EV proteins of *E. faecalis, E. cloacae, L.*
112 *amylovorus, L. reuteri, B. longum* sp. *suis* and *B. fragilis*. Here, 80 µl of each EV sample was
113 mixed with ProteaseMax surfactant (Promega) in 50 mM ammonium bicarbonate to a final
114 concentration of 0.1%. Samples were vortexed for one minute and heated at 95°C for five
115 minutes. Protein reduction and alkylation were performed as reported above. Trypsin digestion
116 was performed in solution.

117 The liquid chromatography and tandem mass spectrometry (LC-MS/MS) analysis was performed
118 using a nanoElute UHPLC coupled to a timsTOFfleX mass spectrometer (Bruker Daltonics,
119 Bremen, Germany) via a CaptiveSpray ion source. Peptides were separated on a 25 cm reversed-
120 phase C18 column (1.6 µm bead size, 120 Å pore size, 75 µm inner diameter, Ion Optics) with a
121 flow rate of 0.3 µl/min and a solvent gradient from 0-35% B in 60 min. Solvent B was 100%
122 acetonitrile in 0.1% formic acid, and solvent A 0.1% formic acid in water. The mass
123 spectrometer was operated in data-dependent Parallel Accumulation-Serial Fragmentation
124 (PASEF) mode. Mass spectra for MS and MS/MS scans were recorded between m/z 100 and
125 1700. Ion mobility resolution was set to 0.85–1.35 V·s/cm over a ramp time of 100 ms. Data-
126 dependent acquisition was performed using 10 PASEF MS/MS scans per cycle with a near 100%
127 duty cycle. A polygon filter was applied in the m/z and ion mobility space to exclude low m/z,
128 singly charged ions from PASEF precursor selection. An active exclusion time of 0.4 min was
129 applied to precursors that reached 20,000 intensity units. Collisional energy was ramped stepwise
130 as a function of ion mobility.

131 Protein identification was performed using the MaxQuant software (versions 2.1.3.0,2.4.3.0 and
132 2.4.7.0) (37). Parameters were set as follows: fixed modification: carbamidomethylation (C),
133 protein N-acetylation, and methionine oxidation as variable modifications. The first search error
134 window of 20 ppm, and mains search error of 4.5 ppm. Trypsin without proline restriction
135 enzyme option was used, with two allowed miscleavages. Minimal unique peptides were set to 1,
136 and the false discovery rate (FDR) allowed was 0.01 (1%) for peptide and protein identification.
137 Species-specific databases were generated from proteomes downloaded from NCBI Genomes. In
138 addition, human, bovine, and pig databases downloaded from Uniprot were included in the
139 MaxQuant searches. The generation of reversed sequences was selected to assign FDR rates.

140 Most of the bacteria were analyzed in three culture replicates. For *F. nucleatum* sp. *animals*, *H.*
141 *biformis, P. russellii*, *S. salivarius* and *T. sanguinis*, the replicates were pooled for LC-MS/MS
142 analysis, due to low signal intensities.

143 ## Prediction of protein cellular localization and function

144 The cellular localization of bEV proteins was predicted using PSORTb version 3.0.3 web server
145 (38) and DeepLocPro (39). Analysis was performed for each species separately, using the default
146 parameters and the species gram type. DeepLocPro predictions were used in cases where
147 PSORTb predictions returned an "unknown". Some of the 50S ribosomal proteins were
148 erroneously predicted as outer membrane or extracellular by DeepLocPro; these were
149 reclassified as cytoplasmic. Eight *V. magna* proteins were predicted by DeepLocPro as cell wall
150 proteins; since gram-negative bacteria do not have an actual cell wall, and these proteins are
151 known to span several envelope layers, they were reclassified as unknown.

152 Protein functions were predicted as clusters of orthologous groups (COG) using eggNOG-
153 mapper v2 (40). Proteins without eggnog annotations were predicted using PANNZER2 (41),
154 converting the Gene Ontology biological functions to COGs using a Python script by Szczerbiak
155 *et al*. (42). Remaining unannotated proteins were processed using the NCBI CD-Search Tool
156 (43).

157 ## Comparative analysis of bacterial extracellular vesicle proteomes

158 To compare bEV proteome compositions across species, we defined protein orthogroups using
159 OrthoFinder v2.5.5 (44) with default parameters. *F. nucleatum* was excluded from this analysis
160 due to the small number of identified proteins. For the quantitative analyses, the remaining data
161 were quantile normalized with the limma R package (45). For inference of the proteome
162 similarity tree and the proteomic versus consensus phylogenetic trees comparison, orthogroup
163 abundances were averaged across replicates by species, and orthogroups with averaged relative
164 abundance values not reaching 0.1% in at least one species were removed to minimize the effect
165 of the total number of identified proteins on tree topology. For the nonmetric multidimensional
166 scaling (nMDS) ordination, orthogroups detected in less than 2 samples were excluded.
167 Orthogroups detected in five out of seven gram-positive species or all of the four remaining
168 gram-negative species were regarded as conserved. The lower threshold value in gram-positive
169 species was chosen due to protein-poor bEV proteomes obtained for *B. suis*, *S. salivarius,* and *T.*
170 *sanguinis* (less than 50 orthogroups identified). The Venn diagrams were created with the eulerr
171 R package (46).

172 For the proteomic similarity tree, bEV proteomes averaged by species were clustered using the
173 Jaccard distance matrix (vegdist function of the vegan package, method = "jaccard", binary =
174 FALSE), with complete linkage as the grouping algorithm (47) and plotted with the dendextend

175 package (48). Branch support was assessed by approximately unbiased (AU) p-values using
176 multiscale bootstrap resampling (49) with 5,000 iterations in the pvclust package (50). This
177 number of iterations ensured accurate estimation of AU p-values (standard errors were less than
178 0.025). The phylogenetic tree for the tanglegram calculation was taken as the phy file from the
179 NCBI Taxonomy Common Tree tool. Before comparison, phylogenetic and proteomic trees were
180 made ultrametric using non-negative least squares with the phangorn package (51). The
181 topological similarity between the proteomic and phylogenetic trees was evaluated using the
182 Fowlkes-Mallows index (52). The index measures the similarity between two dendrograms. It
183 quantifies how similarly the trees are partitioned into clusters, with values of the index ranging
184 from 0 (no similarity) to 1 (perfect agreement). The index estimates the similarity of the
185 compositions of clusters obtained when the trees are split at various numbers of clusters (k). The
186 number of clusters (k) varies from 2 up to (N-1), where (N) is the total number of end branches
187 in each tree (proteomic and phylogenetic). This allows comparison of the overall clustering
188 structure between the two trees. Correspondence between inter-species distances on the trees was
189 measured using the coefficient of cophenetic correlation (53). Fowlkes-Mallows index,
190 cophenetic correlation value, and tanglegrams were calculated and plotted with the dendextend
191 package (48).

192 The proteome ordinations were visualized using nMDS based on Euclidean distances among the
193 samples (vegan package) (47). All plots were drawn with the ggplot2 package (54). Heatmaps
194 were created with the ComplexHeatmap package (55). The values of molecular weight for
195 detected proteins in proteomes were predicted with the Peptides package (56) to test possible
196 correlations with bEV size or gram type.

197 Comparison to fecal extracellular vesicle metaproteomic datasets

198 Peptide-level fecal EV proteome datasets (with protein identifications based on trEMBL) were
199 obtained from the PRIDE repository (accessions PXD045755 and PXD047510) (57, 58).
200 Peptides designated as human were removed. The remaining peptides were analyzed using
201 UniPept (59). We included only those peptides that could be assigned to the genera listed in
202 Table 2 (that is, assigned to the correct bacterial class and not assigned to another order, family,
203 or genus). Average relative intensities were then calculated for unique protein groups. Samples
204 with less than 10 identified protein groups were excluded from further analysis. Protein
205 localizations were predicted from the amino acid sequences available in Uniprot or Uniparc, as
206 described above.

207 # Results

208 ## Morphological characteristics of bEVs

209 Extracellular vesicles were detected in samples of 12 bacterial species by both nanoparticle
210 tracking analysis (NTA) and transmission electron microscopy (TEM). The NTA-based mean
211 bEV diameters ranged from 146–178 nm in gram-positive bacteria and 104–247 nm in gram-
212 negative bacteria (Table 2). The bEV diameters were typically smaller by TEM in comparison to
213 NTA measurements.

214 Based on TEM, most bEVs were likely composed of a single membrane (Fig. 1). A lipid bilayer
215 approximately 8–10 nm thick was visible in most gram-negative bEVs, as well as in
216 *Limosilactobacillus reuteri* and *Turicibacter sanguinis*. In the other samples, the bilayer structure
217 was less distinct. A vesicle with double bilayer membranes was observed in *Enterobacter*
218 *cloacae*. *Veillonella magna* displayed two types of bEVs: large, crumpled vesicles and small,
219 rounded vesicles. In *Streptococcus salivarius*, most objects appeared as chain-like structures with
220 a diameter of 20–25 nm (see top right of the image), compatible with the chains of very small
221 vesicles previously reported in *S. pneumoniae* (60). Electron-dense material was observed in
222 *Bacteroides fragilis, Bifidobacterium longum* sp. *suis, Enterococcus faecalis,* and *Akkermansia*
223 *muciniphila* bEVs, and as central foci inside *L. reuteri* vesicles.

224 In the other eight species, bEVs could not be unequivocally documented, and they were excluded
225 from further analyses. NTA-based bEV concentrations were insufficient for TEM in *E. coli*,
226 *Flavonifactor plautii*, *Floccifex porci*, *Lactobacillus amylovorus,* and *Sutterella parvirubra*. In
227 *Holdemanella biformis* samples, the bEV concentration was not above the level of the negative
228 controls. TEM did not reveal EV-like particles in *Collinsella aerofaciens* and *Clostridium*
229 *leptum*. *C. aerofaciens* exhibited likely protein aggregates without obvious vesicle structure. In
230 *C. leptum* samples, we only observed long fibers with diameters ranging from 2.5–3 nm in the
231 TEM.

232

233 **Table 2. Bacterial extracellular vesicle diameters (nm; mean ± STDEV) and concentrations**
234 **(particles/ml; mean ± STDEV).** NTA: nanoparticle tracking analysis (NTA); TEM:
235 transmission electron microscopy. Brain Heart Infusion broth (BHI) and deMan, Rogosa and
236 Sharpe (MRS) culture media were used as negative controls. The Bacillota phylum was
237 previously Firmicutes.

Phylum	Species	Gram	NTA diam.	TEM diam.	NTA concentration
Actinomycetota	*Bifidobacterium longum sp. suis*	+	131 ± 47	99 ± 56	$1.6 \times 10^{10} \pm 2.5 \times 10^{9}$
Bacillota	*Enterococcus faecalis*	+	146 ± 61	96 ± 34	$1.1 \times 10^{11} \pm 4.3 \times 10^{10}$
Bacillota	*Limosilactobacillus reuteri*	+	143 ± 55	110 ± 41	$2.6 \times 10^{10} \pm 8.5 \times 10^{9}$
Bacillota	*Streptococcus salivarius*	+	124 ± 53	65 ± 19	$1.9 \times 10^{9} \pm 5.1 \times 10^{8}$
Bacillota	*Faecalibacterium prausnitzii*	+	247 ± 105	70 ± 21	$1.7 \times 10^{12} \pm 2.9 \times 10^{11}$
Bacillota	*Peptostreptococcus russellii*	+	104 ± 39	73 ± 16	$2.3 \times 10^{10} \pm 1.9 \times 10^{10}$
Bacillota	*Turicibacter sanguinis*	+	134 ± 55	50 ± 13	$6.5 \times 10^{9} \pm 5.4 \times 10^{9}$
Bacillota	*Veillonella magna*	−	167 ± 66	74 ± 31	$4.2 \times 10^{11} \pm 1.9 \times 10^{11}$
Bacteroidota	*Bacteroides fragilis*	−	150 ± 63	56 ± 19	$7.1 \times 10^{9} \pm 2.1 \times 10^{9}$
Pseudomonadota	*Enterobacter cloacae*	−	146 ± 53	69 ± 21	$5.0 \times 10^{10} \pm 3.9 \times 10^{10}$
Verrucomicrobiota	*Akkermansia muciniphila*	−	178 ± 112	78 ± 24	$8.7 \times 10^{10} \pm 3.2 \times 10^{9}$
Fusobacteria	*Fusobacterium nucleatum sp. animalis*	−	150 ± 64	85 ± 24	$1.9 \times 10^{10} \pm 1.5 \times 10^{10}$
BHI control			138 ± 63	NA	$1.4 \times 10^{9} \pm 1.8 \times 10^{9}$
MRS control			130 ± 61	NA	$6.0 \times 10^{8} \pm 9.2 \times 10^{7}$

238

239

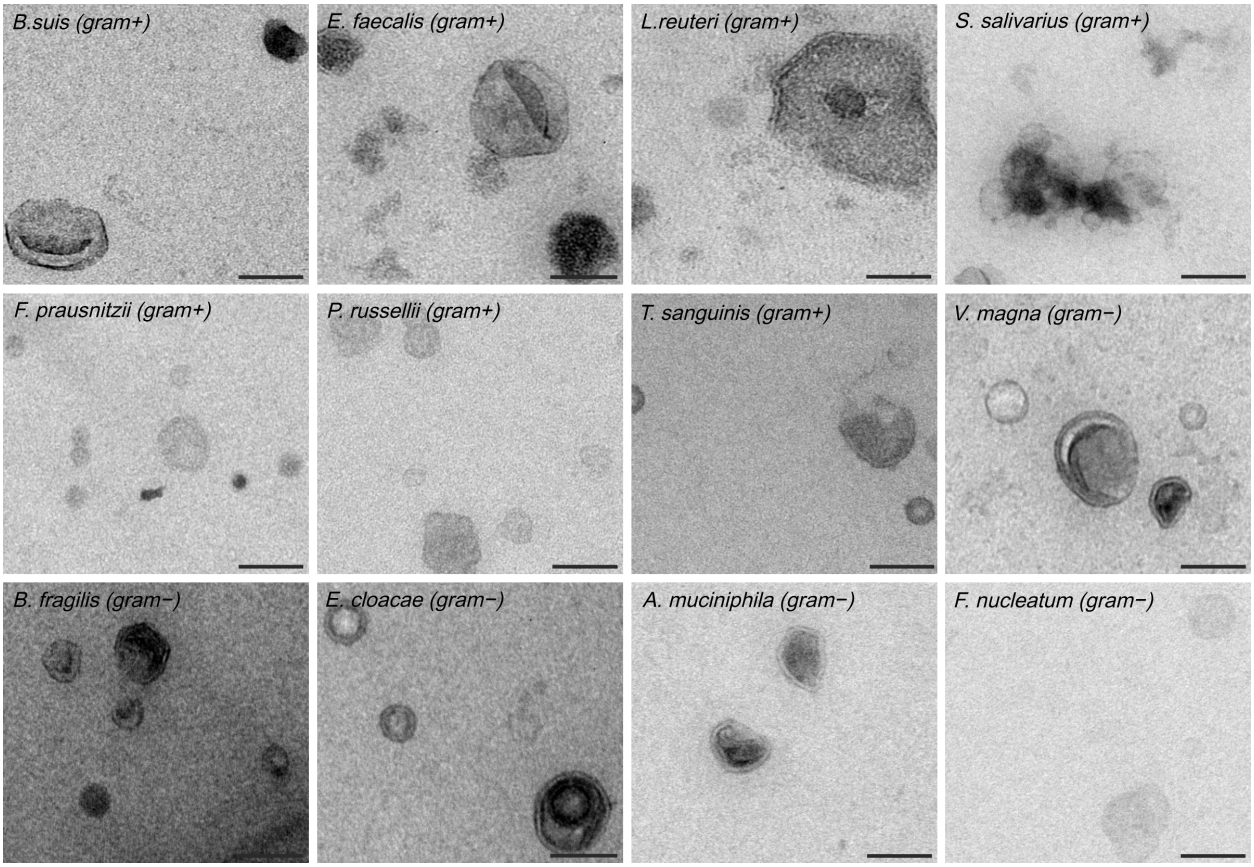

Figure 1. Transmission electron microscopy of extracellular vesicles from gram-positive (+) and gram-negative bacteria (−). Scale bars: 100 nm.

Protein content of bEVs and association of protein diversity with vesicle size

Using high-resolution LC-MS/MS, we identified 17–1297 bacterial proteins per species. These comprised 43–92% of the total MS/MS signal intensity; the remainder were animal proteins most likely derived from the culture media (Table 3). The numbers of identified bacterial proteins were associated with the NTA-measured EV concentrations (Spearman $\rho = 0.59$, $p = 0.049$). In samples with EV concentrations above 2×10^{10} particles/ml (Table 2), the identified bacterial proteins covered 15–49% of the reference proteomes of each species and constituted >85% of all identified proteins and >50% of the total MS/MS intensity (Table 3). In samples with lower EV concentrations, the protein coverages were lower; however, even for *F. nucleatum*, we were able to detect low-abundance proteins down to 0.3% of the total bacterial protein intensity.

The diversity of bacterial proteins (as measured by the numbers of abundant protein orthogroups) was significantly associated with NTA-measured EV diameters (Spearman $\rho = 0.67$; $p = 0.025$).

257 **Table 3. Number of identified bacterial proteins**.

Species	Number of bacterial proteins identified	% of the total number of proteins in samples	% of reference proteome	% of total MS/MS protein intensity
B. longum	63	50	3	9
E. faecalis	1269	92	46	94
L. reuteri	580	87	28	51
S. salivarius	80	46	4	15
F. prausnitzii	1297	94	49	91
P. russellii	526	90	31	50
T. sanguinis	30	43	1	65
V. magna	388	90	20	84
B. fragilis	324	68	8	29
E. cloacae	779	88	15	86
A. muciniphila	512	86	24	76
F. nucleatum	17	63	1	29

258

259 Predicted subcellular localizations of bEV proteins

260 The bacterial proteins identified in gram-positive bEV samples were predicted to be localized in
261 the cytoplasmic membrane, cytoplasm, extracellular space, and cell wall (in the order of median
262 relative abundances; Fig. 2). Gram-negative bEV samples contained proteins from the outer
263 membrane, cytoplasm, extracellular space, periplasm and cytoplasmic membrane. In *F.*
264 *nucleatum* bEVs, periplasmic and extracellular proteins were not observed, possibly due to the
265 low number of identified proteins.

266 *V. magna* bEVs contained a larger share of cytoplasmic membrane and periplasmic proteins than
267 the other gram-negative species, in terms of MS/MS signal intensity (Fig. 2A). Cytoplasmic
268 proteins were relatively abundant in *A. muciniphila* and *F. nucleatum* bEVs. *S. salivarius* and
269 *Peptostreptococcus russellii* bEVs contained a lower share of cytoplasmic membrane proteins
270 compared to other gram-positive species. In *S. salivarius*, >60% of the total intensity consisted of
271 four very abundant glucan-modifying enzymes predicted to be extracellular.

272 The shares of cytoplasmic membrane, cytoplasmic, and periplasmic proteins were generally
273 higher in all species based on the number of identified proteins than by protein intensity (Fig. 2).
274 This indicates a higher diversity of proteins in these compartments in comparison to the
275 extracellular space, cell wall and outer membrane.

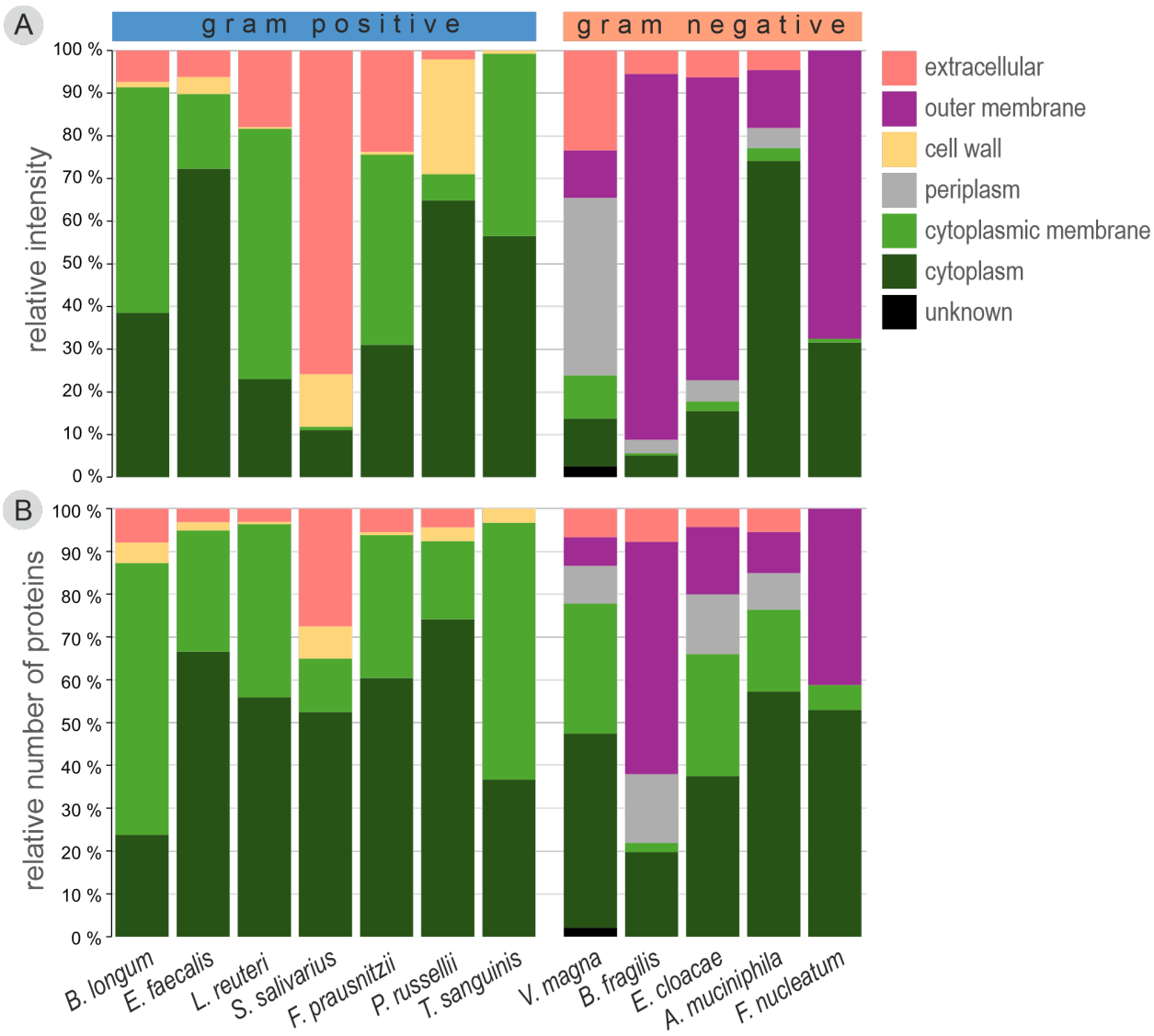

Figure 2. Predicted subcellular localizations of bacterial extracellular vesicle proteins. (A) relative MS/MS intensities; (B) relative numbers of identified proteins.

Predicted functions of bEV proteins

The most prevalent protein functional categories included cell wall/membrane/envelope biogenesis; nutrient transport and metabolism (especially carbohydrates, amino acids, and lipids); energy production and conversion; and translation, ribosomal structure, and biogenesis (Fig. 3). Proteins for RNA and DNA processing were observed in most species. There were no major differences in the predicted protein functional categories of gram-positive and gram-negative bEVs.

Phage proteins were detected in bEVs of several species (Fig. 3). In *E. cloacae*, we observed a high abundance of P2-type temperate phage proteins, with a major capsid protein among the top

289 10 most abundant bEV proteins. Also in *L. reuteri*, a major capsid protein was among the most
290 abundant proteins (>10% of the total bacterial protein intensity).

291 Many of the bEV proteins could not be assigned to a functional category. Among these, the *F.*
292 *prausnitzii* protein WP_015537825.1 (microbial anti-inflammatory molecule, MAM) and the *A.*
293 *muciniphila* proteins WP_197738471.1 (Amuc_1100), and WP_012420447.1 (Amuc_1409) are
294 known to mediate host-microbe interactions (61).

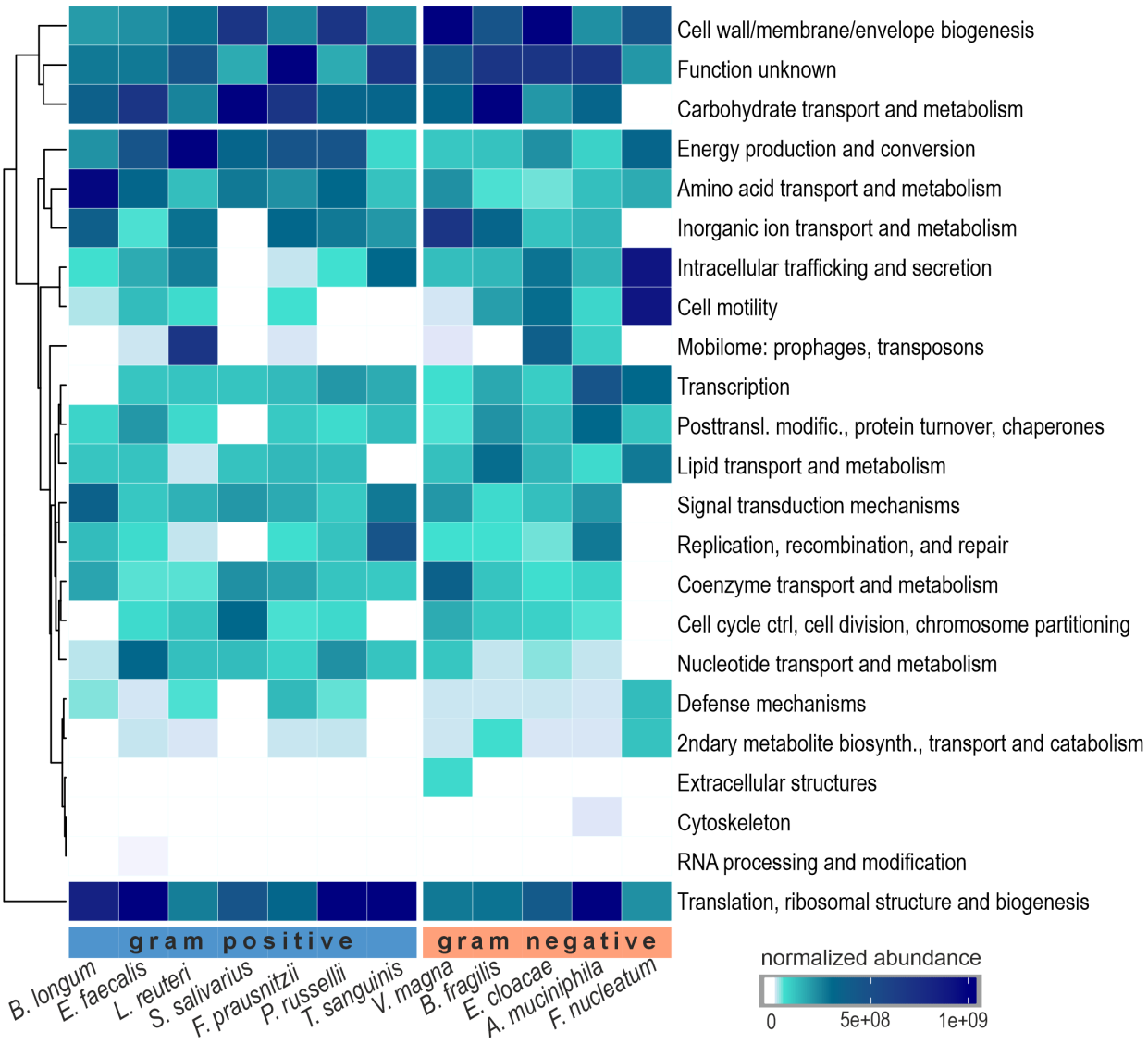

295

296 **Figure 3. Predicted functions of bEV proteins.** The heatmap shows the quantile-normalized
297 total MS/MS intensities of clusters of orthologous groups (COG) functional categories.
298

299

300

301 ## Correlations between bEV proteome compositions, phylogeny and gram type

302 The bEV proteome compositions primarily reflected phylogenetic relationships between the
303 bacterial species (Fig. 4). The *V. magna* proteome grouped with the other Bacillota (Firmicutes)
304 despite the difference in gram type. The cophenetic correlation coefficient between the
305 proteomic and phylogenetic trees was 0.46, indicating a moderate positive correlation between
306 bEV protein composition and bacterial phylogeny. The Fowlkes-Mallows index showed
307 significant non-random similarity between two trees in four out of nine numbers of clusters (two
308 to five clusters); the similarity was random only in one case with nine clusters. Most of the
309 protein orthogroups detected in more than one species (60% of all orthogroups) were shared
310 between gram-positive and gram-negative species. However, *B. longum* of the Actinomycetota
311 grouped with Bacillota, possibly indicating effects of gram type.

312 The *F. nucleatum* proteome was not included in these phylogenetic analyses due to the small
313 number of identified proteins.

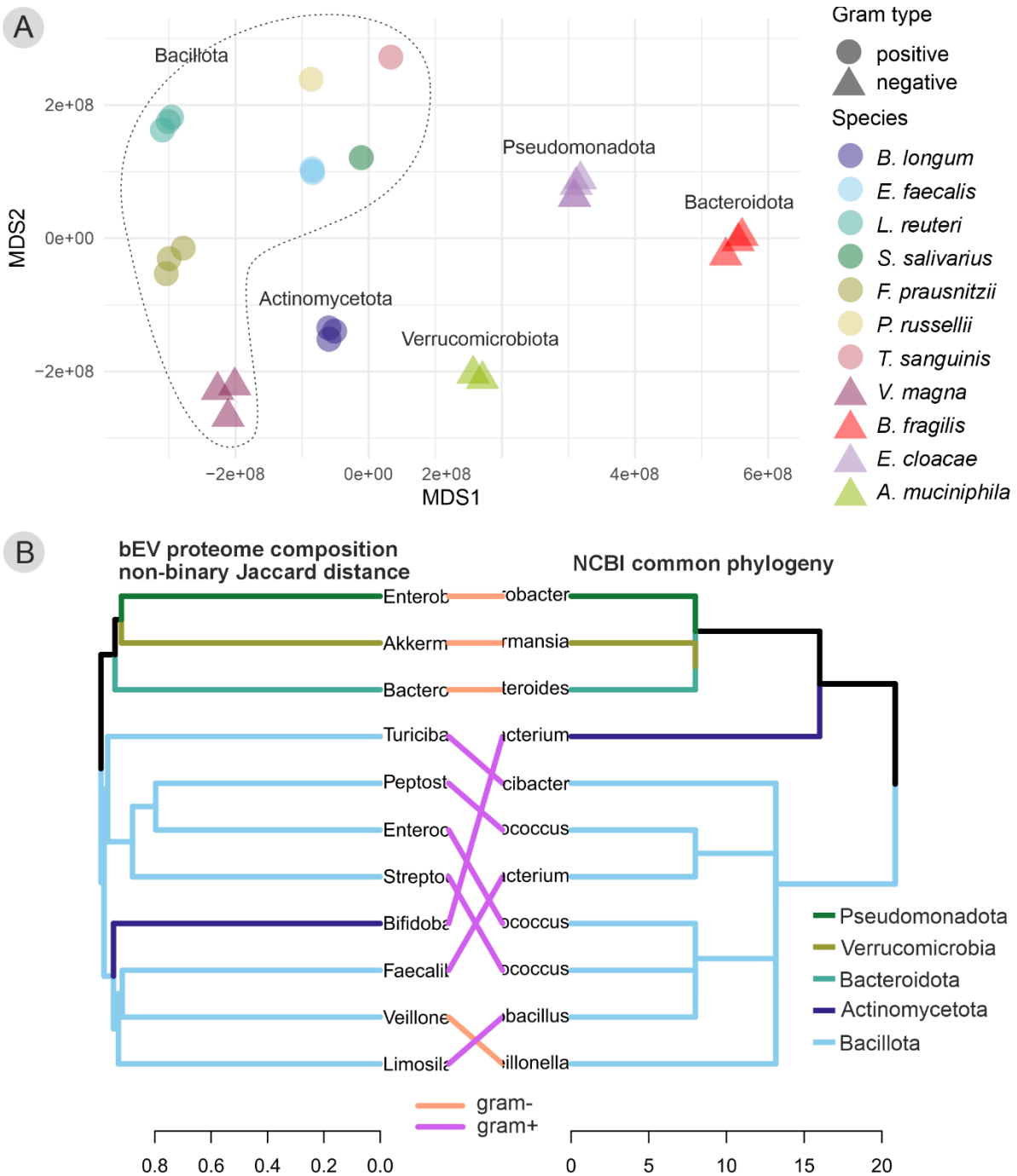

Figure 4. bEV proteome compositions and phylogenetic relationships. (A) nMDS ordination using Euclidean distance matrix of proteome composition (Stress = 0.1). Replicate samples are shown. For some of the species, replicates were pooled to increase LC-MS/MS intensity. The dotted line shows the species of the Bacillota (Firmicutes) phylum. (B) Comparison of proteome composition tree based on bEV protein similarity (complete linkage, non-binary Jaccard distances) and the NCBI common phylogeny tree, which reflects the expected evolutionary relationships derived from nucleotide sequence data. Tree branch colors indicate phyla; connector line colors indicate gram type.

323 ## Conserved and abundant bEV proteins

324 Conserved protein orthogroups were defined as those present in at least five gram-positive
325 species and in four gram-negative species. We identified 14 orthogroups that were conserved in
326 bEVs from both gram-positive and gram-negative bacteria (Fig. 5A). These were predominantly
327 cytoplasmic proteins (Fig. 5B). Glyceraldehyde-3-phosphate dehydrogenase (GAPDH),
328 elongation factor Tu (Ef-Tu), DNA-directed RNA polymerase subunit beta, and several
329 ribosomal proteins had the highest median MS/MS signal intensities. Although these proteins
330 were abundant in some species, the medians were all below 2% of total MS/MS intensity.

331 An additional 29 orthogroups were conserved in gram-positive bEVs only (Fig. 5A). Among all
332 the proteins conserved in gram-positive bEVs, the most abundant were GAPDH, Ef-Tu and
333 PBP1A family penicillin-binding proteins (PBPs).

334 Eighteen orthogroups were conserved in gram-negative bEVs only. The most abundant among
335 all the proteins conserved in gram-negative bEVs included TonB-dependent receptor, S41 family
336 peptidase, GAPDH, DNA-directed RNA polymerase, and some ribosomal proteins. TonB-
337 dependent receptor, BamA/TamA family outer membrane protein assembly factors, and the 30S
338 ribosomal protein S14 were found exclusively in gram-negative bEVs.

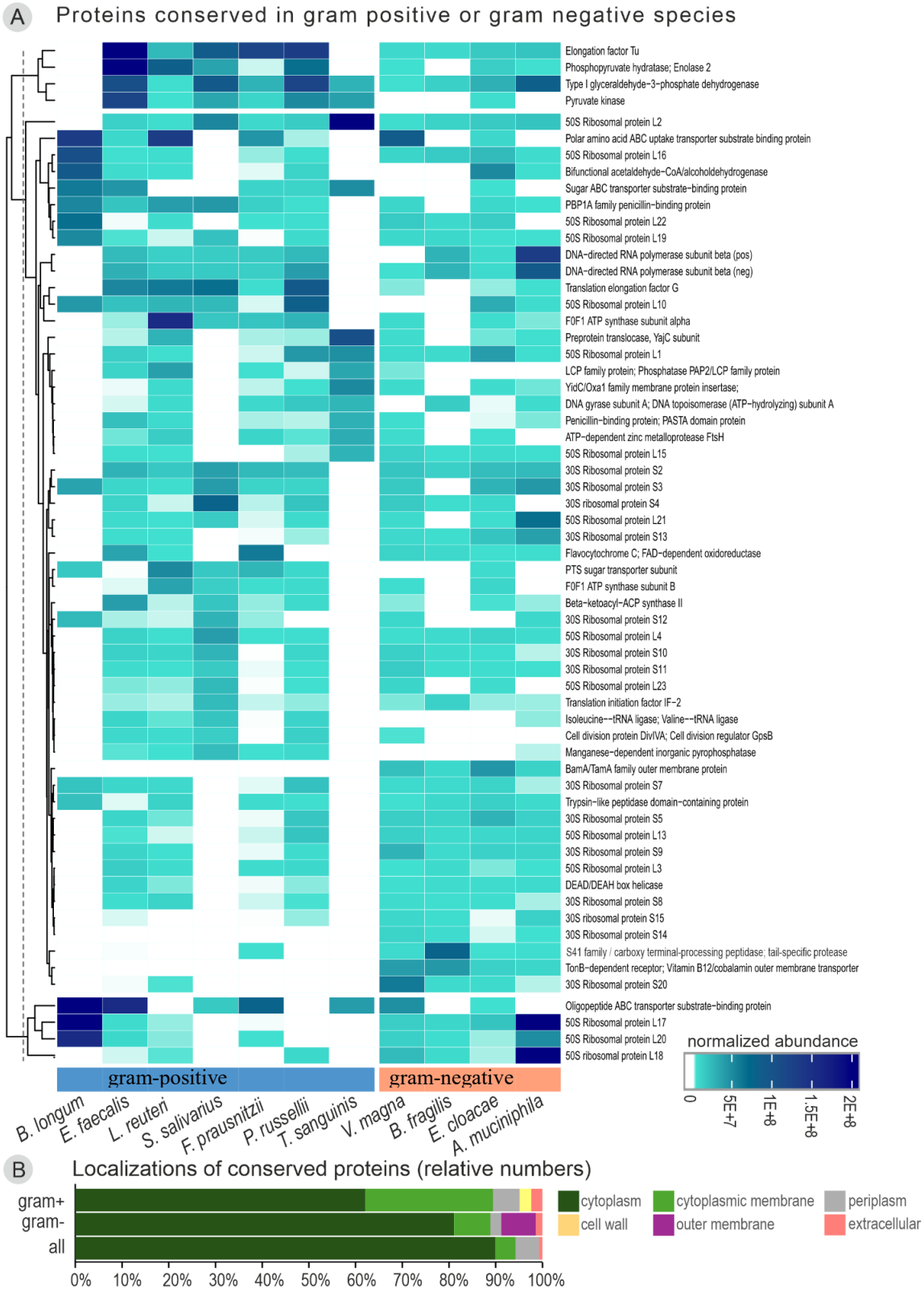

Figure 5. Conserved bEV proteins. A. A heatmap of normalized MS/MS intensities of bEV proteins conserved in gram-positive or gram-negative bacteria. B. The predicted subcellular localizations for bEV proteins conserved in gram-positive bacteria, gram-negative bacteria, and across all species (as relative numbers of identified proteins).

367 We assessed the ten most abundant proteins in each species. A majority of them were species-
368 specific, with only a small proportion shared across several species (Fig. 6A). The top 10
369 proteins accounted for 21–94% of the total MS/MS signal intensity per species and were often
370 predicted to be involved in cell envelope biogenesis, carbohydrate processing or translation;
371 however, in many cases, the functions of these proteins are unknown.

372 In *V. magna*, the most abundant protein was a cobalt chelatase involved in vitamin B_{12}
373 production (Fig. 6A). In *L. reuteri*, the abundant proteins were mostly related to ATP synthesis.
374 *A. muciniphila* bEVs were abundant in chaperonin GroEL, while in *B. longum*, the PBP1A
375 protein dppA accounted for over 23% of total bacterial protein intensity. *T. sanguinis* bEVs were
376 abundant in DNA repair proteins and *P. russellii* bEVs in oxidative stress proteins. Phage
377 components were among the ten most abundant bEV proteins in *L. reuteri* and *E. cloacae*. In *T.*
378 *sanguinis*, >20% of total bacterial protein intensity consisted of a single cytoplasmic membrane
379 protein with unknown function.

380 In gram-positive bEVs, the majority of the most abundant proteins were predicted to be localized
381 in the cytoplasm, cytoplasmic membrane, or the extracellular space (Fig. 6B). In gram-negatives,
382 the most abundant proteins were in outer membrane and cytoplasm, followed by periplasm and
383 the extracellular space (Fig. 6B).

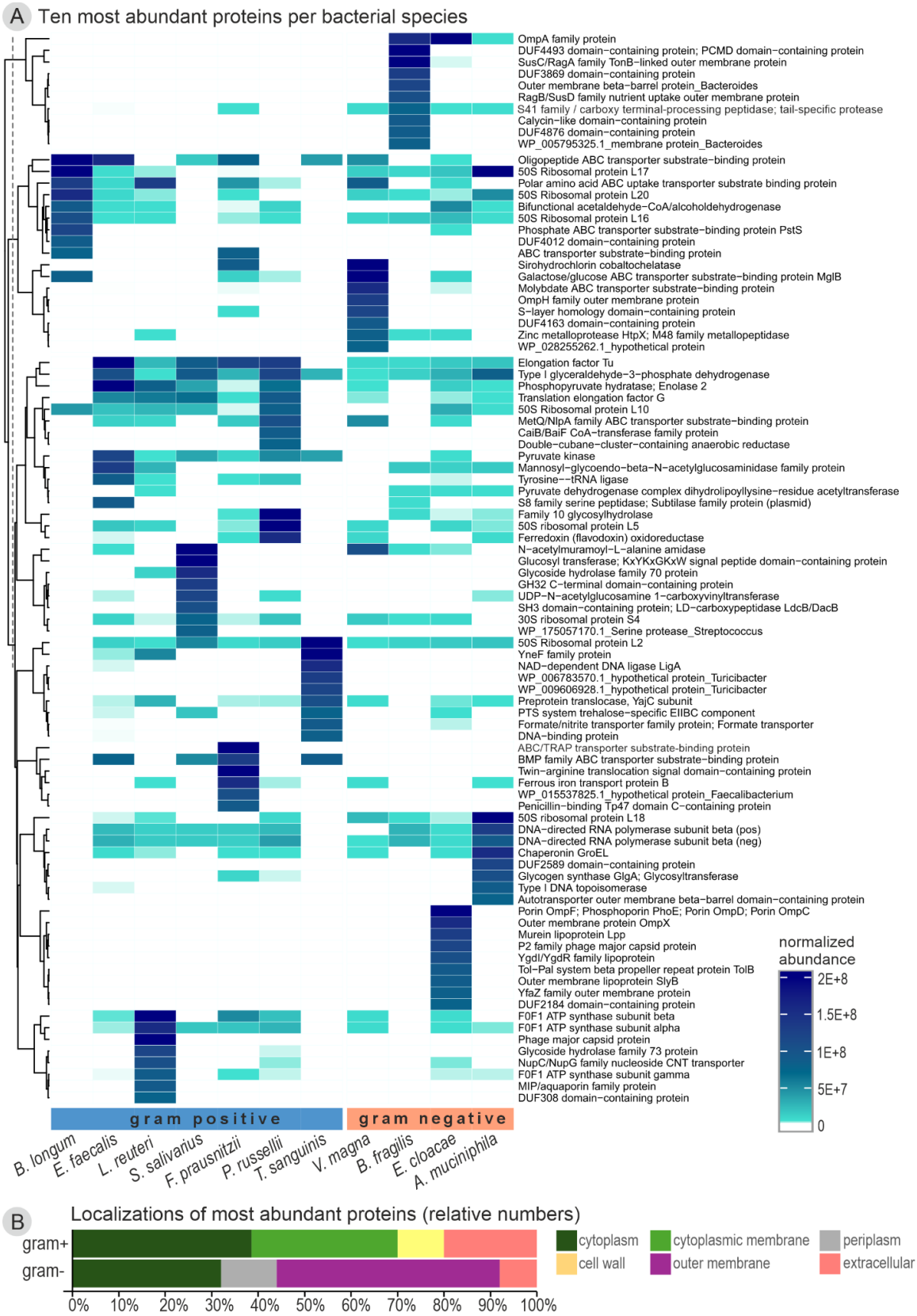

Figure 6. Most abundant bEV proteins. A. Quantile-normalized abundances of proteins which were among the 10 most abundant in at least one bacterial species. B. Predicted subcellular localizations for the most abundant bEV proteins in gram-positive and gram-negative bacteria (as relative numbers of identified proteins).

389 ## Comparison to previously published bEV data

390 We compared our data to previously published *in vitro* bEV proteomics data (available for five
391 species) and fecal EV metaproteomics data (two datasets in which sufficient numbers of peptides
392 could be assigned at the genus level). The bacterial strains and culture media used in the *in vitro*
393 studies differed, except for *E. cloacae*, which was the same strain.

394 In *B. longum,* the subcellular distribution of bEV proteins was similar, despite the difference in
395 the number of identified proteins (63 in our data versus 552 in the previous study) (Fig. 7A)
396 (31). The intensity shares of the major protein functional categories (>5%) were also similar,
397 except for defense mechanisms and the posttranslational modification functional category, which
398 were much less abundant in our data (Fig. 7B).

399 There was also a high degree of similarity in protein subcellular localizations and functional
400 categories in the *E. faecalis* protein datasets (Fig. 7A) (62). With >1100 identified proteins in
401 both datasets, all functional categories with an intensity above 5% matched between the two
402 datasets. The differences in the categories of posttranslational modifications and defense
403 mechanisms were mainly the result of a few individual proteins having higher intensity in either
404 dataset, while the number of proteins per category was similar.

405 For *B. fragilis,* the protein subcellular localizations were relatively similar, with a higher
406 proportion of proteins in the outer membrane and fewer in the periplasmic space in our data (Fig.
407 7A) (27). There was also a good match of functional annotations, with some exceptions (Fig.
408 7B). Carbohydrate transport and metabolism had a lower total number of proteins in our dataset
409 but contained one protein with very high relative intensity (34%) that was not present in the
410 previously published dataset. In the category of amino acid transport, the previously published
411 dataset had only a slightly higher number of proteins, but several of them had higher individual
412 intensities than the sum intensity of all these proteins in our dataset.

413 *E. cloacae* datasets showed the largest variation in protein localizations between our data and
414 previously published data (Fig. 7A) (63). The share of outer membrane proteins was much
415 higher in our data, and extracellular proteins were lower. The functional annotations were similar
416 with two major exceptions (Fig. 7B): cell motility proteins were much more abundant in the
417 previously published dataset, due to the very high intensity (50%) of the flagellin FliC. The cell
418 wall/membrane/envelope biogenesis category was much more abundant in our data, with several
419 outer membrane proteins (Omp) comprising >40% of total intensity.

420 For *F. nucleatum*, we detected a smaller number of proteins than in the previously published
421 dataset (17 versus 98) (64). The share of cytoplasmic proteins was higher and outer membrane
422 proteins lower in our data (Fig. 7A). The relative intensities of several of the functional
423 categories also differed, albeit several with lower intensity still had similar levels in both datasets
424 (Fig. 7B). Major differences in the categories cell motility-intracellular trafficking and
425 posttranslational modification, both consisting of only a few proteins in each dataset, were due to
426 vastly higher intensities of one or two proteins.

427 In the fecal EV metaproteomics data, the localizations of proteins assigned to the genus
428 *Faecalibacterium* (57, 58) were quite similar to our *F. prausnitzii* data, although the fecal data
429 had a higher share of extracellular proteins (Fig. 7A). The fecal *Bacteroides* proteomes (57, 58)
430 contained fewer cytoplasmic and periplasmic proteins than both *in vitro* datasets; this may be in
431 part because conserved proteins often cannot be assigned to a specific genus and were therefore
432 omitted in our analysis. We did not compare the functional annotations to the fecal EV
433 metaproteomics datasets, as species-level annotation was not possible.

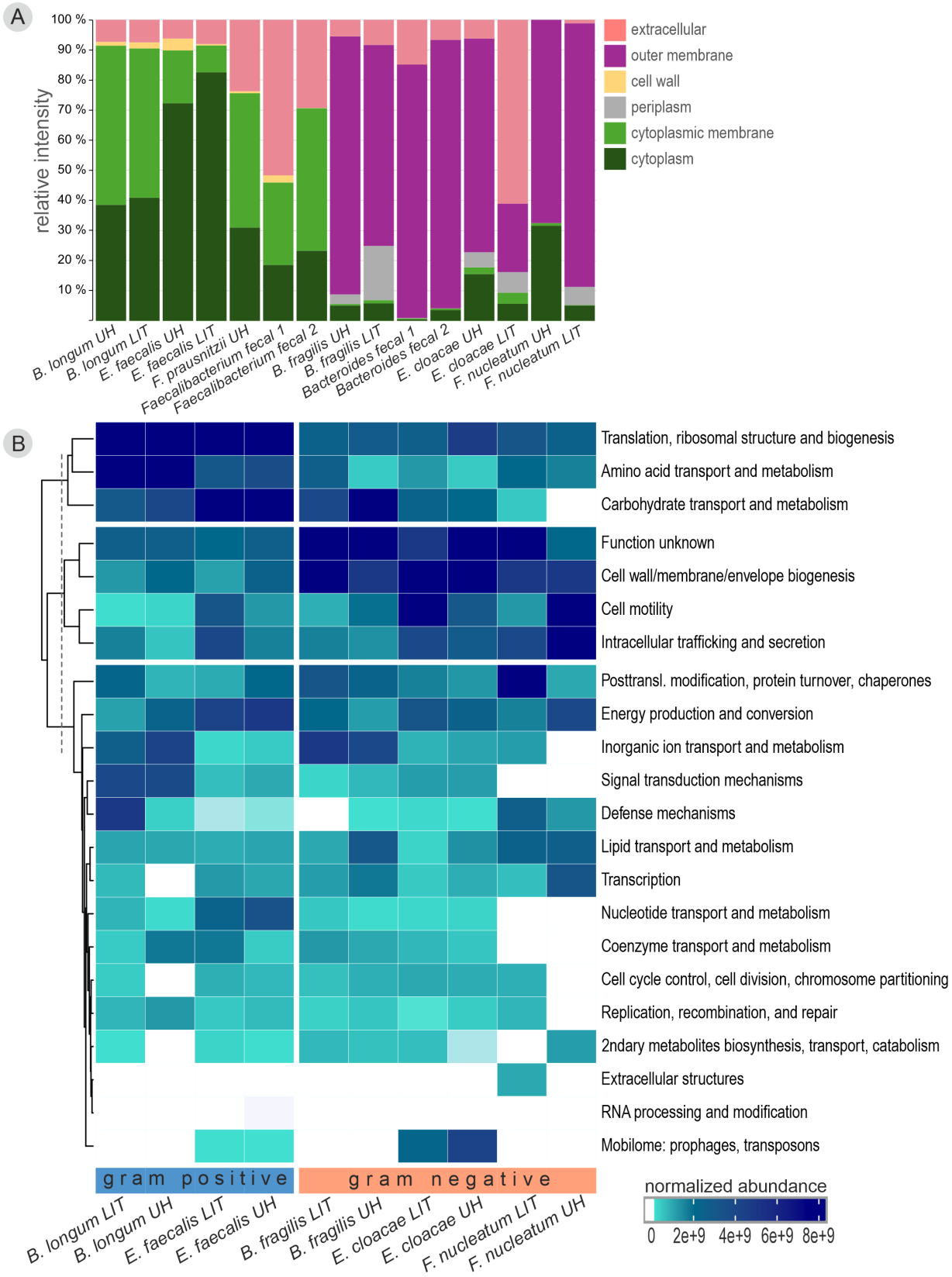

Figure 7. Comparison of predicted subcellular localizations (A) and functions (B) of bEV proteins in our data (UH) and previously published data (LIT; literature). *B. longum (31), E. faecalis* (62), the *Faecalibacterium* genus in fecal metaproteomics data 1 & 2 (57, 58), *B. fragilis* (27), the *Bacteroides* genus in fecal metaproteomics data 1 & 2 (57, 58), *F. nucleatum (64), E. cloacae* (63).

Discussion

We characterized the extracellular vesicle proteomes of 12 commensal bacterial species, representing the six major phyla of the mammalian intestinal microbiota. Predicted protein functions suggest possible roles for commensal bEVs in nutrient processing and host immune system modulation. We identified conserved proteins that may be used as markers for differentiating bacterial versus host EVs. Of note, this is the first report of bEVs secreted by *V. magna*, representing an exceptional class of gram-negative Bacillota (Firmicutes), as well as for *T. sanguinis* and *P. russellii*. We provide the first publicly available proteome of *F. prausnitzii* EVs.

The structures and proteomes of bEVs from gram-positive and gram-negative bacteria reflected the distinct architectures of their parent cells (1). In gram-positive bacteria, a thick peptidoglycan cell wall surrounds the cytoplasmic membrane. They secrete cytoplasmic membrane vesicles (CMVs) by membrane blebbing or explosive cytoplasmic membrane vesicles (ECMVs) by bubbling cell death, through holes degraded in the cell wall (1). In our data, gram-positive bEVs were often irregularly shaped and contained proteins primarily localized to the cytoplasmic membrane and cytoplasm, with varying amounts of extracellular and cell wall proteins.

Gram-negative bacteria have a cytoplasmic membrane and an outer membrane separated by a periplasmic space containing a thin peptidoglycan layer. Here, bEV biogenesis by blebbing produces two types of vesicles: outer membrane vesicles (OMVs), which have a single membrane and periplasmic cargo, but no cytoplasmic cargo; and outer-inner membrane vesicles (OIMVs) with a double membrane and cytoplasmic material. Biogenesis by explosive cell lysis generates explosive OMVs (EOMVs) and explosive OIMVs (EOIMVs), both containing cytoplasmic material, with EOIMVs having more than one vesicle in a larger vesicle (1). In our data, the gram-negative bEVs were mostly spherical with a distinct bilayer membrane, and contained outer membrane, cytoplasmic, extracellular, periplasmic and cytoplasmic membrane proteins. The high share of cytoplasmic proteins suggests biogenesis by explosive cell lysis; thus, the gram-negative bEVs were likely a mixture of EOMVs and OMVs in most cases. *A. muciniphila* samples had a very high abundance of cytoplasmic proteins, in agreement with a previous report (21).

V. magna may produce EVs from both the outer membrane and the cytoplasmic membrane: electron micrographs showed two different types of single-membrane vesicles, and the samples contained equal shares of outer membrane and cytoplasmic membrane proteins. This is

471 unexpected, as gram-negative bacteria are not known to secrete vesicles composed solely of
472 cytoplasmic membrane (1). This warrants further research on EV biogenesis mechanisms in
473 Negativicutes. In *E. cloacae* bEVs, a rare double membrane vesicle was observed, consistent
474 with a previous report (63). Electron-dense material was observed in *B. fragilis* and *A.*
475 *muciniphila* bEVs, and as central foci in *L. reuteri* bEVs, possibly representing cytoplasmic
476 components (65).

477 bEV diameters did not show marked differences between gram types or taxa. They were largely
478 consistent with previous studies, including *B. fragilis* (18), *E. cloacae* (63), *S. salivarius* (66), *B.*
479 *longum* (5), *E. faecalis* (67), *L. reuteri* (68) and *A. muciniphila* (69). Our *F. prausnitzii* bEVs
480 were larger than those reported by Ye et al. (70), which may be due to technical factors such as
481 isolation and purification methods or potential strain differences (71). Electron microscopy
482 typically showed smaller bEV sizes compared to NTA. This may be because NTA measures the
483 hydrodynamic diameters rather than exact membrane-bound dimensions, the lower sensitivity of
484 NTA to small particles, or the shrinkage during the EM fixation (72, 73).

485 Our proteomics data likely covers most of the major bEV proteins, even in the species with the
486 lowest vesicle yields. A 100-nm bEV is expected to contain approximately 4000 protein
487 molecules, based on consensus estimates of cytoplasmic and membrane protein concentrations
488 (74-76). In all proteomes with >60 identified proteins, the intensity ratio of the most abundant vs.
489 least abundant proteins was above 4000, implying that theoretically, we detected down to one
490 molecule per a vesicle. The bEV proteomes with >500 identified proteins covered 15–50% of the
491 reference genomes. However, this represents the pooled proteome of a large number of vesicles,
492 and a single vesicle would probably contain a smaller number of detected proteins. If only
493 proteins with relative intensity above 1/4000 are considered (theoretically representing the
494 protein packaging capacity of a single 100-nm vesicle), the genome coverage was 4–16%. As
495 expected, bEVs with larger diameters were associated with higher diversities of abundant
496 proteins.

497 Functional annotation of bEV proteomes revealed abundant cell envelope-modifying proteins,
498 suggesting involvement in vesicle biogenesis by blebbing. Peptidoglycan biosynthesis and
499 remodeling proteins were present in both gram-positive and gram-negative bEVs, and included
500 Mur ligases and transferases, penicillin-binding proteins (PBPs), and MreB-C rod-shape
501 determining proteins (77, 78). These have been previously reported for bEVs of *E. cloacae* (79)
502 and several other species (80). Bacterial growth and division involve the synthesis of new

503 peptidoglycan and the degradation of old peptidoglycan by hydrolases (78, 81). This creates
504 weakened regions that permit the membrane to bleb from the cell (2, 82). The enrichment of the
505 peptidoglycan biosynthesis and remodeling proteins at sites of active cell wall turnover promotes
506 their incorporation into bEVs (78).

507 Phage-mediated bEV biogenesis has been demonstrated in gram-positive and gram-negative
508 bacteria (1, 83, 84). We identified phage proteins and the recombinase A (RecA) in bEVs from
509 *E. cloacae, L. reuteri*, *A. muciniphila*, *F. prausnitzii*, *E. faecalis,* and *V. magna*. Major capsid
510 proteins were abundant in *E. cloacae* and *L. reuteri* bEVs; small amounts of phage holins were
511 detected in these species and *F. prausnitzii*. Genotoxic stress can activate RecA, which induces
512 the expression of lytic genes such as endolysins and holins from prophages. Holins create holes
513 in the cytoplasmic membrane, allowing endolysins to access and weaken the peptidoglycan
514 layer. This promotes vesicle biogenesis by bubbling cell death in gram-positive bacteria or cell
515 lysis in gram-negative bacteria (83-87). Phage proteins were reported in *E. cloacae* and *E.*
516 *faecalis* bEVs previously (63, 79).

517 Nutrient metabolism and transport proteins were the most common functional group in almost all
518 species, and were often highly abundant. Cobalt chelatase, which is involved in vitamin B_{12}
519 metabolism, was abundant in bEVs of *V. magna* and *F. prausnitzii*. These enzymes provide
520 vitamin B_{12} to other microbes and the host (88). GAPDH, the key glycolytic enzyme with
521 additional roles in iron uptake and membrane trafficking (75, 76, 101), was present in bEVs from
522 most species. Glycoside hydrolases were abundant in *S. salivarius* bEVs and present in lower
523 amounts in other species. They break down complex polysaccharides, providing nutrients for
524 both the producing bacteria and other microbes (11, 89, 90). ABC transporters responsible for
525 the transport of iron, oligopeptides, and amino acids across membranes (10, 91) were abundant
526 in *B. longum* and widely detected across species. TonB-dependent receptors, which facilitate the
527 uptake and delivery of nutrients (10, 92), were found in the bEVs of all gram-negative species.
528 SusC/RagA and SusD/RagB family nutrient uptake outer membrane proteins, involved in the
529 uptake of complex polysaccharides (93), were exclusively detected in *B. fragilis* bEVs.

530 The bEV proteomes of all species included known immunomodulators (61). The elongation
531 factor EF-Tu has cell surface moonlighting functions in adhesion and immune system
532 modulation (94). It was detected in bEVs from nine species and was particularly abundant in *E.*
533 *faecalis* and *P. russellii*. The OmpA outer membrane porin family of commensal bacteria can
534 promote intestinal homeostasis by inducing IL-22 (95). They were present in all gram-negative

535 bEV samples, with high abundances in *E. cloacae* and *B. fragilis*. The *F. prausnitzii* microbial
536 anti-inflammatory molecule (MAM) downregulates NF-κB signaling in epithelial cells (96, 97).
537 The chaperonin/heat shock protein GroEL, known for its immunoregulatory activity (98), was
538 especially abundant in *A. muciniphila* bEVs. The *A. muciniphila* bEVs also contained less
539 abundant proteins that have been reported to modulate gut barrier integrity (99), epithelial stem
540 cells (100) and GLP-1 secretion (101).

541 The functions of many abundant bEV proteins are unknown, especially in *T. sanguinis*, *F.*
542 *prausnitzii*, and *B. fragilis*. This limits our understanding of the potential roles of bEVs and
543 encourages experimental studies on these proteins.

544 The bEV proteome compositions primarily reflected phylogenetic relationships of the producing
545 bacteria. This was especially evident in the *V. magna* bEV proteome, which clustered with other
546 Bacillota bEVs despite the difference in gram type. Thus, bEVs largely inherit the proteome
547 compositions of their parent cells, regardless of the differences in biogenesis mechanisms. This
548 suggests the majority of proteins were loaded into bEVs non-selectively.

549 To identify potential markers differentiating bEVs from host EVs, we assessed for conserved
550 bEV proteins. Although the majority of the abundant bEV proteins were species-specific, we
551 detected 14 orthologous proteins in the bEVs of most gram-positive and gram-negative bacteria.
552 These were primarily predicted to be cytoplasmic, and as such, not ideal as universal bEV
553 markers, since OMVs of gram-negative bacteria lack cytoplasmic proteins (1). The most
554 abundant of the broadly conserved bEV proteins included Ef-Tu, GAPDH, DNA-directed RNA
555 polymerase subunit beta, and certain ribosomal proteins. EF-Tu is listed among the top 50 most
556 conserved bEV proteins deposited in the EVpedia database (102) and may be partially localized
557 on the cell surface (94). GAPDH has been proposed as a target for vaccines against bacterial
558 infections due to its abundance, partial membrane localization, involvement in virulence, and
559 limited homology with host GAPDH (103). The 30S ribosomal protein S4 was found in most
560 bacterial species and does not have mitochondrial orthologues present in animal EVs.

561 TonB-dependent receptor was the most prevalent outer-membrane protein and is a potential
562 marker for gram-negative bEVs. BamA/TamA family outer membrane protein and 30S
563 ribosomal protein S14 were also exclusively detected in gram-negative bEVs, although less
564 abundant. PBP1A is a potential marker for gram-positive bEVs, although related proteins were
565 also present in some gram-negative bEVs.

566 bEV proteomes are likely affected by experimental methods, bacterial growth conditions, and the
567 strain of the producing bacteria (1). However, the predicted localization patterns of proteins
568 observed in our study were consistent with those reported in the literature, including *in vitro*
569 bEVs from *F. nucleatum* (64), *B. fragilis* (27), and *E. faecalis* (62), as well as *Bacteroides* and
570 *Faecalibacterium* proteomes extracted from fecal EV metaproteomes (57, 58). This suggests that
571 the types of bEVs obtained from different experimental procedures, growth conditions, and
572 bacterial strains are reproducible. The lower proportion of cytoplasmic proteins detected in the
573 fecal bEV data may be attributed to their conserved nature, which prevents the assignment of
574 peptides to specific taxa.

575 There was also a general similarity in the predicted functions between our proteomic data and
576 previously published *in vitro* data. This was particularly evident in *E. faecalis* bEVs, with both
577 studies detecting large numbers of proteins (62). In other species, observed differences were
578 mostly due to individual proteins present at highly different intensities. For example, our *B.*
579 *fragilis* data included a highly abundant outer membrane protein with unknown function that was
580 absent in the previous study (27).

581 In some species, we detected fewer proteins compared to the literature datasets, likely due to low
582 bEV concentrations. *B. longum* bEVs contained considerably fewer proteins in our study (31).
583 This probably affected the detection of proteins of the smaller functional categories, although the
584 intensity shares of the subcellular localizations and the major functional categories were similar.
585 For *F. nucleatum* bEVs, despite differences in culture media, strain, and the very low number of
586 identified proteins in our dataset, there were similarities in both cellular localization patterns and
587 the distribution of protein functional categories (64).

588 Limitations of the work

589 The culture conditions were not optimized for each species, as we used a standardized protocol,
590 and the growth phases of the cultures were not controlled. These may affect the yields, types, and
591 compositions of bEVs (104). The observed bEV concentrations probably do not indicate the EV
592 production capacity of these species *in vivo*. In bEV extraction, we used a 0.22 µm filter, which
593 may have excluded some of the larger bEVs, but it was necessary to reliably remove bacterial
594 cells. Protein amounts injected in LC-MS/MS were not equalized, as we aimed for maximal
595 resolution for each species. The number of identified bacterial proteins is therefore not directly

596 comparable between species, but the relative ratios of the subcellular localizations and main
597 functional categories can be compared.

598 Conclusions

599 Our study provides an overview of commensal bEV proteomes across the major phyla of the
600 mammalian intestinal microbiota.

601 The bEV compositions reflected the envelope structures of gram-positive and gram-negative
602 bacteria. The gram-negative Bacillota *V. magna* (and possibly other Negativicutes) may have an
603 exceptional ability to produce both outer membrane and cytoplasmic membrane vesicles.
604 Peptidoglycan modifying enzymes observed in several species and bacteriophage proteins very
605 abundant in *E. cloacae* and *L. reuteri,* probably mediate bEV biogenesis.

606 Commensal bEVs are likely involved in nutrient metabolism and transport as well as in the
607 modulation of the host immune system. The functions of many abundant bEV proteins are
608 unknown.

609 Elongation factor Tu and GAPDH are potential generic markers for bEVs. TonB-dependent
610 receptors and PBP1A may be used as markers for gram-negative and gram-positive bEVs,
611 respectively.

612 Our comparison to previous bEV studies suggests that bEV structures and their proteomic
613 profiles are largely reproducible, despite differences in bacterial growth conditions, bEV
614 isolation protocols, and analysis methods.

615 ## Author contributions

616 **RNM**: data analysis (lead), visualization (supporting), writing (lead). **AM**: proteomics and NTA
617 data analysis (lead), visualization (lead), writing (supporting). **TPM**: data analysis and writing
618 (supporting). **MK**: TEM and NTA data analysis and writing (supporting). **JM:** proteomics
619 laboratory analysis (supporting), writing (supporting) **MS**: proteomics laboratory analysis (lead),
620 writing (supporting). **MH**: bacterial strains (supporting), writing (supporting). **AK**:
621 metaproteomics data analysis (supporting), writing (supporting). **SM:** methodology and writing
622 (supporting). **JR:** resources, conceptualization and writing (supporting). **TRL**: resources and
623 writing (supporting). **TAN**: proteomics laboratory analysis (lead), proteomics data analysis and
624 writing (supporting). **MN**: conceptualization, funding acquisition, methodology, resources,
625 supervision, writing (lead), data analysis, visualization (supporting).

626 ## Acknowledgments

627 We thank chief laboratory technician Kirsi Lahti for performing bacterial culture, and Dr. Ulla
628 Hynönen, Dr. Silja Åvall-Jääskeläinen, Dr. Kaisa Hiippala, Dr. Reetta Satokari and prof. Willem
629 de Vos for expert consultation. We acknowledge the services of the University of Helsinki: the
630 EV Core Facility in Viikki for EV isolation and NTA analysis, the HiPREP Core in the FIMM
631 Technology Centre supported by HiLIFE and Biocenter Finland for electron microscopy, the
632 Electron Microscopy Unit of the Institute of Biotechnology for providing the facilities, the
633 Clinical Microbiology Laboratory of the Veterinary Teaching Hospital (YESLAB) for the
634 MALDI identifications of the *in vitro* cultured bacteria, and the DNA Sequencing and Genomics
635 Laboratory (supported by HiLIFE and Biocenter Finland funding), Institute of Biotechnology for
636 DNA sequencing.

637 Mass spectrometry-based proteomic analyses were performed by the Proteomics Core Facility,
638 Department of Immunology, University of Oslo/Oslo University Hospital, which is supported by
639 the Core Facilities program of the South-Eastern Norway Regional Health Authority. The core
640 facility is a member of the National Network of Advanced Proteomics Infrastructure (NAPI),
641 funded by the Research Council of Norway INFRASTRUKTUR-program (project number:
642 295910).

643 ## Disclosure of interest

644 *The authors report no conflict of interest.*

645 # References

646 1. Toyofuku M, Schild S, Kaparakis-Liaskos M, Eberl L. Composition and functions of bacterial
647 membrane vesicles. Nature reviews Microbiology. 2023;21(7):415-30. doi: 10.1038/s41579-023-00875-
648 5.
649 2. Schwechheimer C, Kuehn MJ. Outer-membrane vesicles from Gram-negative bacteria:
650 biogenesis and functions. Nature reviews Microbiology. 2015;13(10):605-19. doi: 10.1038/nrmicro3525.
651 3. Brown L, Wolf JM, Prados-Rosales R, Casadevall A. Through the wall: extracellular vesicles in
652 Gram-positive bacteria, mycobacteria and fungi. Nature reviews Microbiology. 2015;13(10):620-30. doi:
653 10.1038/nrmicro3480.
654 4. Tarashi S, Zamani MS, Omrani MD, Fateh A, Moshiri A, Saedisomeolia A,… Kubow S. Commensal
655 and pathogenic bacterial-derived extracellular vesicles in host-bacterial and interbacterial dialogues: two
656 sides of the same coin. Journal of Immunology Research. 2022;2022(1):8092170. doi:
657 10.1155/2022/8092170.
658 5. Morishita M, Sagayama R, Yamawaki Y, Yamaguchi M, Katsumi H, Yamamoto A. Activation of
659 Host Immune Cells by Probiotic-Derived Extracellular Vesicles via TLR2-Mediated Signaling Pathways.
660 Biological & pharmaceutical bulletin. 2022;45(3):354-9. doi: 10.1248/bpb.b21-00924.
661 6. Beveridge TJ. Structures of gram-negative cell walls and their derived membrane vesicles.
662 Journal of bacteriology. 1999;181(16):4725-33. doi: 10.1128/JB.181.16.4725-4733.1999.
663 7. Liu Y, Defourny KAY, Smid EJ, Abee T. Gram-positive bacterial extracellular vesicles and their
664 impact on health and disease. Frontiers in microbiology. 2018;9:1502. doi: 10.3389/fmicb.2018.01502.
665 8. Díaz-Garrido N, Badia J, Baldomà L. Microbiota-derived extracellular vesicles in interkingdom
666 communication in the gut. J Extracell Vesicles. 2021;10(13):e12161. doi: 10.1002/jev2.12161.
667 9. Gul L, Modos D, Fonseca S, Madgwick M, Thomas JP, Sudhakar P,… Korcsmaros T. Extracellular
668 vesicles produced by the human commensal gut bacterium Bacteroides thetaiotaomicron affect host
669 immune pathways in a cell-type specific manner that are altered in inflammatory bowel disease. Journal
670 of Extracellular Vesicles. 2022;11(1):e12189. doi: 10.1002/jev2.12189.
671 10. Juodeikis R, Carding SR. Outer membrane vesicles: biogenesis, functions, and issues.
672 Microbiology and Molecular Biology Reviews : MMBR. 2022;86(4):e00032-22. doi:
673 10.1128/mmbr.00032-22.
674 11. Rakoff-Nahoum S, Coyne MJ, Comstock LE. An ecological network of polysaccharide utilization
675 among human intestinal symbionts. Current Biology. 2014;24(1):40-9. doi: 10.1016/j.cub.2013.10.077.
676 12. Erttmann SF, Swacha P, Aung KM, Brindefalk B, Jiang H, Härtlova A, . . . Gekara NO. The gut
677 microbiota prime systemic antiviral immunity via the cGAS-STING-IFN-I axis. Immunity. 2022;55(5):847-
678 61. doi: 10.1016/j.immuni.2022.04.006.
679 13. Li M, Lee K, Hsu M, Nau G, Mylonakis E, Ramratnam B. Lactobacillus-derived extracellular
680 vesicles enhance host immune responses against vancomycin-resistant enterococci. BMC microbiology.
681 2017;17(1):1-8. doi: 10.1186/s12866-017-0977-7.
682 14. Fábrega M-J, Rodríguez-Nogales A, Garrido-Mesa J, Algieri F, Badía J, Giménez R,… Baldomà L.
683 Intestinal anti-inflammatory effects of outer membrane vesicles from Escherichia coli Nissle 1917 in DSS-
684 experimental colitis in mice. Frontiers in Microbiology. 2017;8:1274. doi: 10.3389/fmicb.2017.01274.
685 15. Hiippala K, Barreto G, Burrello C, Diaz-Basabe A, Suutarinen M, Kainulainen V,… Eklund KK. Novel
686 Odoribacter splanchnicus strain and its outer membrane vesicles exert immunoregulatory effects in
687 vitro. Frontiers in microbiology. 2020;11:575455. doi: 10.3389/fmicb.2020.575455.
688 16. Seo MK, Park EJ, Ko SY, Choi EW, Kim S. Therapeutic effects of kefir grain Lactobacillus-derived
689 extracellular vesicles in mice with 2,4,6-trinitrobenzene sulfonic acid-induced inflammatory bowel
690 disease. Journal of Dairy Science. 2018;101(10). doi: 10.3168/jds.2018-15014.
691 17. Alvarez C-S, Badia J, Bosch M, Giménez R, Baldomà L. Outer membrane vesicles and soluble
692 factors released by probiotic Escherichia coli Nissle 1917 and commensal ECOR63 enhance barrier
693 function by regulating expression of tight junction proteins in intestinal epithelial cells. Frontiers in
694 microbiology. 2016;7:1981. doi: 10.3389/fmicb.2016.01981.

18. Gilmore WJ, Johnston EL, Bitto NJ, Zavan L, O'Brien-Simpson N, Hill AF, Kaparakis-Liaskos M. Bacteroides fragilis outer membrane vesicles preferentially activate innate immune receptors compared to their parent bacteria. Frontiers in Immunology. 2022;13:970725. doi: 10.3389/fimmu.2022.970725.
19. Liu C, Yazdani N, Moran CS, Salomon C, Seneviratne CJ, Ivanovski S, Han P. Unveiling clinical applications of bacterial extracellular vesicles as natural nanomaterials in disease diagnosis and therapeutics. Acta Biomaterialia. 2024;180. doi: 10.1016/j.actbio.2024.04.022.
20. Humaira, Ahmad I, Shakir HA, Khan M, Franco M, Irfan M. Bacterial extracellular vesicles: potential therapeutic applications, challenges, and future prospects. Journal of Basic Microbiology. 2024;64(10):e2400221. doi: 10.1002/jobm.202400221.
21. Zhao S, Xiang J, Abedin M, Wang J, Zhang Z, Zhang Z,… Xiao J. Characterization and Anti-Inflammatory Effects of Akkermansia muciniphila-Derived Extracellular Vesicles. Microorganisms. 2025;13(2):464. doi: 10.3390/microorganisms13020464.
22. Zheng T, Hao H, Liu Q, Li J, Yao Y, Liu Y,… Yi H. Effect of extracelluar vesicles derived from Akkermansia muciniphila on intestinal barrier in colitis mice. Nutrients. 2023;15(22):4722. doi: 10.3390/nu15224722.
23. Chelakkot C, Choi Y, Kim D-K, Park HT, Ghim J, Kwon Y,… Gho YS. Akkermansia muciniphila-derived extracellular vesicles influence gut permeability through the regulation of tight junctions. Experimental & molecular medicine. 2018;50(2):e450-e. doi: 10.1038/emm.2017.282.
24. Chen Y, Ou Z, Pang M, Tao Z, Zheng X, Huang Z,… Chen P. Extracellular vesicles derived from Akkermansia muciniphila promote placentation and mitigate preeclampsia in a mouse model. Journal of Extracellular Vesicles. 2023;12(5):12328. doi: 10.1002/jev2.12328.
25. Hong M-G, Song E-J, Yoon HJ, Chung W-H, Seo HY, Kim D,… Kim SI. Clade-specific extracellular vesicles from Akkermansia muciniphila mediate competitive colonization via direct inhibition and immune stimulation. Nature Communications. 2025;16(1):2708. doi: 10.1038/s41467-025-57631-x.
26. Ashrafian F, Shahriary A, Behrouzi A, Moradi HR, Keshavarz Azizi Raftar S, Lari A,… Khatami S. Akkermansia muciniphila-derived extracellular vesicles as a mucosal delivery vector for amelioration of obesity in mice. Frontiers in microbiology. 2019;10:2155. doi: 10.3389/fmicb.2019.02155.
27. Zakharzhevskaya NB, Vanyushkina AA, Altukhov IA, Shavarda AL, Butenko IO, Rakitina DV,… Kulikov EE. Outer membrane vesicles secreted by pathogenic and nonpathogenic Bacteroides fragilis represent different metabolic activities. Scientific reports. 2017;7(1):5008. doi: 10.1038/s41598-017-05264-6.
28. Chen C, He Y-Q, Gao Y, Pan Q-W, Cao J-S. Extracellular vesicles of Bacteroides fragilis regulated macrophage polarization through promoted Sema7a expression. Microbial Pathogenesis. 2024;187:106527. doi: 10.1016/j.micpath.2023.106527.
29. Ferreira TG, Trindade CNdR, Bell P, Teixeira-Ferreira A, Perales JE, Vommaro RC,… Ferreira EdO. Identification of the alpha-enolase P46 in the extracellular membrane vesicles of Bacteroides fragilis. Memorias do Instituto Oswaldo Cruz. 2018;113(3):178-84. doi: 10.1590/0074-02760170340.
30. Nishiyama K, Takaki T, Sugiyama M, Fukuda I, Aiso M, Mukai T,… Okada N. Extracellular vesicles produced by Bifidobacterium longum export mucin-binding proteins. Applied and environmental microbiology. 2020;86(19):e01464-20. doi: 10.1128/AEM.01464-20.
31. Mandelbaum N, Zhang L, Carasso S, Ziv T, Lifshiz-Simon S, Davidovich I,… Cooks T. Extracellular vesicles of the Gram-positive gut symbiont Bifidobacterium longum induce immune-modulatory, anti-inflammatory effects. npj Biofilms and Microbiomes. 2023;9(1):30. doi: 10.1038/s41522-023-00400-9.
32. Stentz R, Jones E, Juodeikis R, Wegmann U, Guirro M, Goldson AJ,… Brown IR. The proteome of extracellular vesicles produced by the human gut bacteria Bacteroides thetaiotaomicron in vivo is influenced by environmental and host-derived factors. Applied and Environmental Microbiology. 2022;88(16):e00533-22. doi: 10.1128/aem.00533-22.
33. Yu MSC, Chiang DM, Reithmair M, Meidert A, Brandes F, Schelling G,… Zenner C. The proteome of bacterial membrane vesicles in Escherichia coli—a time course comparison study in two different media. Frontiers in Microbiology. 2024;15:1361270. doi: 10.3389/fmicb.2024.1361270.

34. Van Deun J, Mestdagh P, Agostinis P, Akay Ö, Anand S, Anckaert J,… Consortium E-T. EV-TRACK: transparent reporting and centralizing knowledge in extracellular vesicle research. Nature Methods. 2017;14(3):228-32. doi: 10.1038/nmeth.4185.
35. König E, Sali V, Heponiemi P, Salminen S, Valros A, Junnikkala S, Heinonen M. Herd-level and individual differences in fecal lactobacilli dynamics of growing pigs. Animals. 2021;11(1):113. doi: 10.3390/ani11010113.
36. Puhka M, Nordberg ME, Valkonen S, Rannikko A, Kallioniemi O, Siljander P, Af Hällström TM. KeepEX, a simple dilution protocol for improving extracellular vesicle yields from urine. European journal of pharmaceutical sciences. 2017;98:30-9. doi: 10.1016/j.ejps.2016.10.021.
37. Cox J, Mann M. MaxQuant enables high peptide identification rates, individualized p.p.b.-range mass accuracies and proteome-wide protein quantification. Nature Biotechnology. 2008;26(12):1367-72. doi: 10.1038/nbt.1511.
38. Yu NY, Wagner JR, Laird MR, Melli G, Rey S, Lo R,… Foster LJ. PSORTb 3.0: improved protein subcellular localization prediction with refined localization subcategories and predictive capabilities for all prokaryotes. Bioinformatics. 2010;26(13):1608-15. doi: 10.1093/bioinformatics/btq249.
39. Moreno J, Nielsen H, Winther O, Teufel F. Predicting the subcellular location of prokaryotic proteins with DeepLocPro. Bioinformatics. 2024;40(12):btae677. doi: 10.1093/bioinformatics/btae677.
40. Cantalapiedra CP, Hernández-Plaza A, Letunic I, Bork P, Huerta-Cepas J. eggNOG-mapper v2: functional annotation, orthology assignments, and domain prediction at the metagenomic scale. Molecular Biology and Evolution. 2021;38(12):5825-9. doi: 10.1093/molbev/msab293.
41. Törönen P, Holm L. PANNZER—a practical tool for protein function prediction. Protein Science. 2022;31(1):118-28. doi: 10.1002/pro.4193.
42. Szczerbiak P, Szydlowski LM, Wydmański W, Renfrew PD, Koehler Leman J, Kosciolek T. Large protein databases reveal structural complementarity and functional locality. bioRxiv. 2024:2024-08.
43. Marchler-Bauer A, Bo Y, Han L, He J, Lanczycki CJ, Lu S,… Gonzales NR. CDD/SPARCLE: functional classification of proteins via subfamily domain architectures. Nucleic acids research. 2017;45(D1):D200-D3. doi: 10.1093/nar/gkw1129.
44. Emms DM, Kelly S. OrthoFinder: phylogenetic orthology inference for comparative genomics. Genome biology. 2019;20(1):1-14. doi: 10.1186/s13059-019-1832-y.
45. Ritchie ME, Phipson B, Wu DI, Hu Y, Law CW, Shi W, Smyth GK. limma powers differential expression analyses for RNA-sequencing and microarray studies. Nucleic acids research. 2015;43(7):e47-e. doi: 10.1093/nar/gkv007.
46. Larsson J. eulerr: Area-Proportional Euler and Venn Diagrams with Ellipses. R package version 7.0.2; 2024.
47. Oksanen J, Blanchet FG, Friendly M, Kindt R, Legendre P, McGlinn D,… Solymos P. vegan: Community Ecology Package. R package version 2.5-6. 2019.
48. Galili T. dendextend: an R package for visualizing, adjusting and comparing trees of hierarchical clustering. Bioinformatics. 2015;31(22):3718-20. doi: 10.1093/bioinformatics/btv428.
49. Shimodaira H. Approximately unbiased tests of regions using multistep-multiscale bootstrap resampling. The Annals of Statistics. 2004;32(6). doi: 10.1214/009053604000000823.
50. Suzuki R, Shimodaira H. Pvclust: an R package for assessing the uncertainty in hierarchical clustering. Bioinformatics. 2006;22(12):1540-2. doi: 10.1093/bioinformatics/btl117.
51. Schliep KP. phangorn: phylogenetic analysis in R. Bioinformatics. 2011;27(4):592-3. doi: 10.1093/bioinformatics/btq706.
52. Fowlkes EB, Mallows CL. A method for comparing two hierarchical clusterings. Journal of the American statistical association. 1983;78(383):553-69. doi: 10.1080/01621459.1983.10478008.
53. Sokal RR, Rohlf FJ. The comparison of dendrograms by objective methods. Taxon. 1962;11(2):33-40. doi: 10.2307/1217208.
54. Wickham H. ggplot2: Elegant Graphics for Data Analysis: Springer-Verlag New York; 2016.
55. Gu Z. Complex heatmap visualization. Imeta. 2022;1(3):e43. doi: 10.1002/imt2.43.
56. Osorio D, Rondón-Villarreal P, Torres R. Peptides: a package for data mining of antimicrobial peptides. The R Journal. 2015;7(1):4-14. doi: 10.32614/RJ-2015-001.

57. Kaisanlahti A, Turunen J, Byts N, Samoylenko A, Bart G, Virtanen N,… Reunanen J. Maternal microbiota communicates with the fetus through microbiota-derived extracellular vesicles. Microbiome. 2023;11(1):249. doi: 10.1186/s40168-023-01694-9.
58. Mishra S, Tejesvi MV, Hekkala J, Turunen J, Kandikanti N, Kaisanlahti A,… Reunanen J. Gut microbiome-derived bacterial extracellular vesicles in patients with solid tumours. Journal of Advanced Research. 2025;68:375-86. doi: 10.1016/j.jare.2024.03.003.
59. Vande Moortele T, Devlaminck B, Van de Vyver S, Van Den Bossche T, Martens L, Dawyndt P,… Verschaffelt P. Unipept in 2024: Expanding Metaproteomics Analysis with Support for Missed Cleavages and Semitryptic and Nontryptic Peptides. Journal of Proteome Research. 2025;24(2):949-54. doi: 10.1021/acs.jproteome.4c00848.
60. Mehanny M, Koch M, Lehr C-M, Fuhrmann G. Streptococcal extracellular membrane vesicles are rapidly internalized by immune cells and alter their cytokine release. Frontiers in immunology. 2020;11:80. doi: 10.3389/fimmu.2020.00080.
61. Balint D, Brito IL. Human-gut bacterial protein-protein interactions: understudied but impactful to human health. Trends in Microbiology. 2024;32(4):325-32. doi: 10.1016/j.tim.2023.09.009.
62. Costantini PE, Vanpouille C, Firrincieli A, Cappelletti M, Margolis L, Ñahui Palomino RA. Extracellular vesicles generated by gram-positive bacteria protect human tissues ex vivo from HIV-1 infection. Frontiers in Cellular and Infection Microbiology. 2022;11:822882. doi: 10.3389/fcimb.2021.822882.
63. Bhar S, Edelmann MJ, Jones MK. Characterization and proteomic analysis of outer membrane vesicles from a commensal microbe, Enterobacter cloacae. Journal of proteomics. 2021;231:103994. doi: 10.1016/j.jprot.2020.103994.
64. Liu J, Hsieh C-L, Gelincik O, Devolder B, Sei S, Zhang S,… Chang Y-F. Proteomic characterization of outer membrane vesicles from gut mucosa-derived fusobacterium nucleatum. Journal of proteomics. 2019;195:125-37. doi: 10.1016/j.jprot.2018.12.029.
65. Pérez-Cruz C, Delgado L, López-Iglesias C, Mercade E. Outer-inner membrane vesicles naturally secreted by gram-negative pathogenic bacteria. PLoS one. 2015;10(1):e0116896. doi: 10.1371/journal.pone.0116896.
66. Kulig K, Kowalik K, Surowiec M, Karnas E, Barczyk-Woznicka O, Zuba-Surma E,… Karkowska-Kuleta J. Isolation and characteristics of extracellular vesicles produced by probiotics: yeast Saccharomyces boulardii CNCM I-745 and bacterium Streptococcus salivarius K12. Probiotics and Antimicrobial Proteins. 2024;16(3):936-48. doi: 10.1007/s12602-023-10085-3.
67. Ma RY, Deng ZL, Du QY, Dai MQ, Luo YY, Liang YE,… Zhao WH. Enterococcus faecalis extracellular vesicles promote apical periodontitis. Journal of Dental Research. 2024;103(6):672-82. doi: 10.1177/00220345241230867.
68. Dean SN, Leary DH, Sullivan CJ, Oh E, Walper SA. Isolation and characterization of Lactobacillus-derived membrane vesicles. Scientific reports. 2019;9(1):877. doi: 10.1038/s41598-018-37120-6.
69. Kang C-s, Ban M, Choi E-J, Moon H-G, Jeon J-S, Kim D-K,… Kim Y-K. Extracellular Vesicles Derived from Gut Microbiota, Especially Akkermansia muciniphila, Protect the Progression of Dextran Sulfate Sodium-Induced Colitis. PLoS ONE. 2013 Oct 24;8(10). doi: 10.1371/journal.pone.0076520.
70. Ye L, Wang Y, Xiao F, Wang X, Li X, Cao R,… Zhang T. F. prausnitzii-derived extracellular vesicles attenuate experimental colitis by regulating intestinal homeostasis in mice. Microbial cell factories. 2023;22(1):235. doi: 10.1186/s12934-023-02243-7.
71. Rodovalho VdR, da Luz BSR, Nicolas A, Jardin J, Briard-Bion V, Folador EL,… Azevedo VAdC. Different culture media and purification methods unveil the core proteome of Propionibacterium freudenreichii-derived extracellular vesicles. Microlife. 2023;4:uqad029. doi: 10.1093/femsml/uqad029.
72. Van der Pol E, Coumans FAW, Grootemaat AE, Gardiner C, Sargent IL, Harrison P,… Nieuwland R. Particle size distribution of exosomes and microvesicles determined by transmission electron microscopy, flow cytometry, nanoparticle tracking analysis, and resistive pulse sensing. Journal of Thrombosis and Haemostasis. 2014;12(7):1182-92. doi: 10.1111/jth.12602.

73. Noble JM, Roberts LM, Vidavsky N, Chiou AE, Fischbach C, Paszek MJ,… Kourkoutis LF. Direct comparison of optical and electron microscopy methods for structural characterization of extracellular vesicles. Journal of structural biology. 2020;210(1):107474. doi: 10.1016/j.jsb.2020.107474.
74. Dolgalev GV, Safonov TA, Arzumanian VA, Kiseleva OI, Poverennaya EV. Estimating total quantitative protein content in Escherichia coli, Saccharomyces cerevisiae, and HeLa Cells. International Journal of Molecular Sciences. 2023;24(3):2081. doi: 10.3390/ijms24032081.
75. Milo R. What is the total number of protein molecules per cell volume? A call to rethink some published values. Bioessays. 2013;35(12):1050-5. doi: 10.1002/bies.201300066.
76. Wishart DS, et al. E. coli Statistics. Escherichia coli Metabolome Database. 2025.
77. Galinier A, Delan-Forino C, Foulquier E, Lakhal H, Pompeo F. Recent advances in peptidoglycan synthesis and regulation in bacteria. Biomolecules. 2023;13(5):720. doi: 10.3390/biom13050720.
78. Miyachiro MM, Contreras-Martel C, Dessen A. Penicillin-binding proteins (PBPs) and bacterial cell wall elongation complexes. Macromolecular protein complexes II: structure and function. 2019:273-89. doi: 10.1007/978-3-030-28151-9_8.
79. Afonina I, Tien B, Nair Z, Matysik A, Lam LN, Veleba M,… Wenk M. The composition and function of Enterococcus faecalis membrane vesicles. Microlife. 2021;2:uqab002. doi: 10.1093/femsml/uqab002.
80. Briaud P, Carroll RK. Extracellular vesicle biogenesis and functions in gram-positive bacteria. Infection and immunity. 2020;88(12):10-1128. doi: 10.1128/iai.00433-20.
81. Deatherage BL, Lara JC, Bergsbaken T, Barrett SLR, Lara S, Cookson BT. Biogenesis of bacterial membrane vesicles. Molecular microbiology. 2009;72(6):1395-407. doi: 10.1111/j.1365-2958.2009.06731.x.
82. Toyofuku M, Nomura N, Eberl L. Types and origins of bacterial membrane vesicles. Nature Reviews Microbiology. 2019;17(1):13-24. doi: 10.1038/s41579-018-0112-2.
83. da Silva Barreira D, Lapaquette P, Novion Ducassou J, Couté Y, Guzzo J, Rieu A. Spontaneous Prophage Induction Contributes to the Production of Membrane Vesicles by the Gram-Positive Bacterium Lacticaseibacillus casei BL23. mBio. 2022;13(5):e02375-22. doi: 10.1128/mbio.02375-22.
84. Baeza N, Delgado L, Comas J, Mercade E. Frontiers | Phage-Mediated Explosive Cell Lysis Induces the Formation of a Different Type of O-IMV in Shewanella vesiculosa M7T. Frontiers in Microbiology. 2021/10/08;12. doi: 10.3389/fmicb.2021.713669.
85. Turnbull L, Toyofuku M, Hynen AL, Kurosawa M, Pessi G, Petty NK,… Shimoni R. Explosive cell lysis as a mechanism for the biogenesis of bacterial membrane vesicles and biofilms. Nature communications. 2016;7(1):11220. doi: 10.1038/ncomms11220.
86. Toyofuku M, Zhou S, Sawada I, Takaya N, Uchiyama H, Nomura N. Membrane vesicle formation is associated with pyocin production under denitrifying conditions in P seudomonas aeruginosa PAO 1. Environmental Microbiology. 2014;16(9):2927-38. doi: 10.1111/1462-2920.12260.
87. Cahill J, Young R. Phage lysis: multiple genes for multiple barriers. Advances in virus research. 2019;103:33-70. doi: 10.1016/bs.aivir.2018.09.003.
88. Juodeikis R, Jones E, Deery E, Beal DM, Stentz R, Kräutler B,… Warren MJ. Nutrient smuggling: Commensal gut bacteria-derived extracellular vesicles scavenge vitamin B12 and related cobamides for microbe and host acquisition. Journal of Extracellular Biology. 2022;1(10):e61. doi: 10.1002/jex2.61.
89. Tian C-m, Yang M-f, Xu H-m, Zhu M-z, Zhang Y, Yao J,… Li D-f. Emerging role of bacterial outer membrane vesicle in gastrointestinal tract. Gut Pathogens. 2023;15(1):20. doi: 10.1186/s13099-023-00543-2.
90. Elhenawy W, Debelyy MO, Feldman MF. Preferential packing of acidic glycosidases and proteases into Bacteroides outer membrane vesicles. mBio. 2014;5(2):10-1128. doi: 10.1128/mBio.00909-14.
91. Köster W. ABC transporter-mediated uptake of iron, siderophores, heme and vitamin B12. Research in microbiology. 2001;152(3-4):291-301. doi: 10.1016/s0923-2508(01)01200-1.
92. Bolam DN, van den Berg B. TonB-dependent transport by the gut microbiota: novel aspects of an old problem. Current opinion in structural biology. 2018;51:35-43. doi: 10.1016/j.sbi.2018.03.001.

897 93. Pollet RM, Martin LM, Koropatkin NM. TonB-dependent transporters in the Bacteroidetes:
898 unique domain structures and potential functions. Molecular Microbiology. 2021;115(3):490-501. doi:
899 10.1111/mmi.14683.
900 94. Harvey KL, Jarocki VM, Charles IG, Djordjevic SP. The diverse functional roles of elongation factor
901 Tu (EF-Tu) in microbial pathogenesis. Frontiers in microbiology. 2019;10:2351. doi:
902 10.3389/fmicb.2019.02351.
903 95. Wang Y, Ngo VL, Zou J, Gewirtz AT. Commensal bacterial outer membrane protein A induces
904 interleukin-22 production. Cell reports. 2024;43(6). doi: 10.1016/j.celrep.2024.114292.
905 96. Quévrain E, Maubert MA, Michon C, Chain F, Marquant R, Tailhades J,… Pigneur B. Identification
906 of an anti-inflammatory protein from Faecalibacterium prausnitzii, a commensal bacterium deficient in
907 Crohn's disease. Gut. 2016;65(3):415-25. doi: 10.1136/gutjnl-2014-307649.
908 97. Auger S, Kropp C, Borras-Nogues E, Chanput W, Andre-Leroux G, Gitton-Quent O,… Langella P.
909 Intraspecific diversity of microbial anti-inflammatory molecule (MAM) from Faecalibacterium prausnitzii.
910 International Journal of Molecular Sciences. 2022;23(3):1705. doi: 10.3390/ijms23031705.
911 98. Al-Nedawi K, Mian MF, Hossain N, Karimi K, Mao YK, Forsythe P,… Bienenstock J. Gut commensal
912 microvesicles reproduce parent bacterial signals to host immune and enteric nervous systems. The
913 FASEB Journal. 2015;29(2):684-95. doi: 10.1096/fj.14-259721.
914 99. Post SE, Brito IL. Structural insight into protein–protein interactions between intestinal
915 microbiome and host. Current Opinion in Structural Biology. 2022;74:102354. doi:
916 10.1016/j.sbi.2022.102354.
917 100. Kang E-J, Kim J-H, Kim YE, Lee H, Jung KB, Chang D-H,… Lee C-H. The secreted protein
918 Amuc_1409 from Akkermansia muciniphila improves gut health through intestinal stem cell regulation.
919 Nature Communications. 2024;15(1):2983. doi: 10.1038/s41467-024-47275-8.
920 101. Yoon HS, Cho CH, Yun MS, Jang SJ, You HJ, Kim J-h,… Lee K. Akkermansia muciniphila secretes a
921 glucagon-like peptide-1-inducing protein that improves glucose homeostasis and ameliorates metabolic
922 disease in mice. Nature microbiology. 2021;6(5):563-73. doi: 10.1038/s41564-021-00880-5.
923 102. Kim DK, Kang B, Kim OY, Choi Ds, Lee J, Kim SR,… Jang SC. EVpedia: an integrated database of
924 high-throughput data for systemic analyses of extracellular vesicles. Journal of extracellular vesicles.
925 2013;2(1):20384. doi: 10.3402/jev.v2i0.20384.
926 103. Perez-Casal J, Potter AA. Glyceradehyde-3-phosphate dehydrogenase as a suitable vaccine
927 candidate for protection against bacterial and parasitic diseases. Vaccine. 2016;34(8):1012-7. doi:
928 10.1016/j.vaccine.2015.11.072.
929 104. Zavan L, Bitto NJ, Johnston EL, Greening DW, Kaparakis-Liaskos M. Helicobacter pylori growth
930 stage determines the size, protein composition, and preferential cargo packaging of outer membrane
931 vesicles. Proteomics. 2019;19(1-2):1800209. doi: 10.1002/pmic.201800209.